Bosonization and density-matrix renormalization group studies of the Fulde-Ferrell-Larkin-Ovchinnikov phase and irrational magnetization plateaus in coupled chains

G. Roux,[1,*] E. Orignac,[2,†] P. Pujol,[1] and D. Poilblanc[1]
[1]*Laboratoire de Physique Théorique, Université Paul Sabatier, CNRS, 118 Route de Narbonne, 31400 Toulouse, France*
[2]*Laboratoire de Physique de l'Ecole Normale Supérieure de Lyon, CNRS, 46 Allée d'Italie, 69007 Lyon, France*
(Revised manuscript received 15 October 2006; published 20 June 2007)

We review the properties of two coupled fermionic chains, or ladders, under a magnetic field parallel to the lattice plane. Results are computed by complementary analytical (bosonization) and numerical (density-matrix renormalization group) methods, which allows a systematic comparison. Limiting cases such as coupled-band and coupled-chain regimes are discussed. We particularly focus on the evolution of the superconducting correlations under increasing field and on the presence of irrational magnetization plateaus. We found the existence of large doping-dependent magnetization plateaus in the weakly interacting and strong-coupling limits and in the nontrivial case of isotropic couplings. We report on the existence of extended Fulde-Ferrell-Larkin-Ovchinnikov phases [Phys. Rev. **135**, A550 (1964); Sov. Phys. JETP **20**, 762 (1965);] within the isotropic *t-J* and Hubbard models, deduced from the evolution of different observables under magnetic field. Emphasis is put on the variety of superconducting order parameters present at high magnetic field. We have also computed the evolution of the Luttinger exponent corresponding to the ungapped spin mode appearing at finite magnetization. In the coupled-chain regime, the possibility of having polarized triplet pairing under high field is predicted by bosonization.

DOI: 10.1103/PhysRevB.75.245119 PACS number(s): 71.10.Pm, 74.20.Mn, 74.81.−g, 75.40.Mg

I. INTRODUCTION

Low-dimensional strongly correlated systems have attracted strong interest in the last years because fluctuations and energetic competitions drive these systems into exotic phases. Quasi-one-dimensional or strongly anisotropic two-dimensional superconductors are also known to be good candidates for the realization of Fulde-Ferrell-Larkin-Ovchinnikov (FFLO) phases[1–4] because the orbital effects of the magnetic field, which induce the H_{c2} critical field in type-II superconductors, can be strongly suppressed. In a singlet superconductor without orbital effect, there is a competition between polarizing the spins of the electrons and binding them into Cooper pairs, leading to a theoretical critical field called the Pauli limit or the paramagnetic limit.[2–5] However, this limit can be exceeded with an inhomogeneous order parameter (FFLO) which can be energetically favorable, allowing pockets of polarized electrons and paired electrons. Qualitatively, the FFLO mechanism consists in giving singlet Cooper pairs a finite momentum, which leads to this inhomogeneous superconducting order parameter. Among these intriguing low-dimensional systems, ladders, which consist of a few coupled chains, proved to display deep new physical behaviors and sustained considerable experimental and theoretical work.[6]

At half-filling, ladders are Mott insulators and have a spin gap if the number of chains is even (this gap goes to zero in the limit of an infinite number of coupled chains) and no spin gap if it is odd. The two-leg ladder has thus a spin-liquid ground state with exponentially decaying magnetic correlations. Spin gaps can also open under magnetic field for rational values of the magnetization per site, leading to plateaus in the magnetization curve.[7] Experimental evidence of zero magnetization plateaus have been reported on ladder and coupled-dimer compounds[8–10] such as $Cu_2(C_5H_{12}N_2)_2Cl_4$, $(C_5H_{12}N)_2CuBr_4$, and $(5IAP)_2CuBr_4 \cdot 2H_2O$. Away from half-filling, a few systems are known to develop irrational magnetization plateaus controlled by hole concentration.[11–13] Furthermore, when holes are introduced into the spin-liquid two-leg ladder, these charge carriers generically bring the system into either a metallic or a superconducting state. The isotropic two-leg ladder is known to have a wide superconducting phase[14,15] and also a metallic phase with dominant charge-density wave[16] (CDW) fluctuations. Another interesting feature is the appearance of commensurate CDW for a commensurate hole concentration.[16] The theoretically proposed framework to account for superconductivity in doped ladders relies on magnetic fluctuations and is based on the resonating-valence-bond (RVB) mechanism for superconductivity proposed by Anderson in the context of high-T_c superconductors.[17] Within the isotropic Hubbard and *t-J* models, singlet pairing with an unconventional modified *d*-wave structure is found. The competition[18] between superconductivity and CDW has indeed been observed in the copper oxide ladder compound $Sr_{14-x}Ca_xCu_{24}O_{41+\delta}$ (SCCO) for which the superconducting state only appears under high pressure.[19] However, the mechanism responsible for superconductivity in SCCO has not reached a full agreement yet. In this context, the upper critical magnetic fields determined from transport measurements[20,21] suggest that the Pauli limit is exceeded in SCCO, which reassesses the issue of the nature of the pairing. Note that superconductivity has been discovered in the zigzag ladder subsystem of the copper oxide compound $Pr_2Ba_4Cu_7O_{15-\delta}$ at ambient pressure.[22]

Recently, a superconducting two-leg *t-J* ladder under a strong magnetic field in the plane of the ladder was studied numerically[23] using the density-matrix renormalization group[24,25] (DMRG) method. The magnetic curve displays a doping-dependent magnetization plateau, as predicted[26] by

Cabra *et al.* for a Hubbard ladder. In addition to this nontrivial magnetic behavior, an exceeding of the Pauli limit was found. Within the *t-J* model, this exceeding of the Pauli limit was explained by a one-dimensional analog of the FFLO phase, hence reconciling the expectation of singlet pairing and the exceeding of the Pauli limit. Lastly, the behavior of the superconducting correlations studied in Ref. 23 showed a surprising behavior in and outside the plateau with a notable emergence of $S^z=0$ triplet superconducting correlations.

In this paper, we propose that Ref. 23 can be greatly completed by an extensive comparison of bosonization and numerical calculations and by extending the results to discuss the case of weakly interacting or strongly anisotropic ladders and also to the case of weakly coupled chains. In particular, we show that the picture developed in Ref. 23 is consistent with bosonization and extends to both Hubbard and *t-J* models, supporting its generality. While most studies on the FFLO phase resort to mean-field theories for low-dimensional and unconventional superconductors,[4] we use here approaches which are more relevant for quasi-one-dimensional strongly correlated systems. In the same spirit, an early study on the superconducting phase of the *t-J* chain which gave evidence of developing FFLO-like correlations[27] was based on exact diagonalization computations, and bosonization has also been used in this context[28] on an attractive Hubbard system.

The paper is organized as follows: First, after introducing microscopic models (Sec. II), we briefly examine the noninteracting and strong-coupling limits in Sec. III where large doping-dependent magnetization plateaus can occur. The coupled-band regime is discussed in detail in Sec. IV and corresponds to the case of doped isotropic ladders, which is the most studied at zero magnetic field. Lastly, the coupled-chain regime is studied under magnetic field (Sec. V).

II. MICROSCOPIC MODELS AND CONVENTION

We describe the ladder system with a standard one-orbital Hubbard model which can have different hopping terms along the chains ($\|$) and between the chains ($\perp$). We consider a situation where no magnetic orbital effect is present and thus only keep a Zeeman coupling to the spin degree of freedom. This would experimentally correspond to the situation where the magnetic field H is in the plane of the ladder (and even along the direction of the ladder to minimize all orbital effects). Then, one can write the Hubbard Hamiltonian

$$\mathcal{H} = -t_{\|} \sum_{i,p=1,2,\sigma} [c^{\dagger}_{i+1,p,\sigma} c_{i,p,\sigma} + \text{H.c.}] - t_{\perp} \sum_{i,\sigma} [c^{\dagger}_{i,2,\sigma} c_{i,1,\sigma} + \text{H.c.}] + U \sum_{i,p=1,2} n_{i,p,\uparrow} n_{i,p,\downarrow} - \sum_{i,p=1,2} H \cdot \mathbf{S}_{i,p}, \quad (1)$$

where $c^{\dagger}_{i,p,\sigma}$, $\mathbf{S}_{i,p}$, and $n_{i,p,\sigma}$ are, respectively, electron creation, spin, and density operators at site i on chain p and σ is the spin index. The $g\mu_B$ prefactor has been absorbed in the definition of H for convenience. Free band dispersion is given by

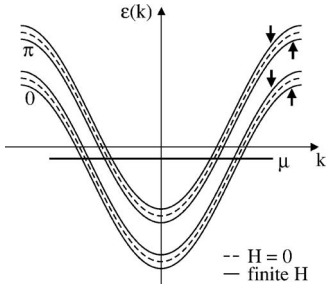

FIG. 1. Splitting of the band dispersion in a noninteracting doped ladder (μ is the chemical potential) due to Zeeman effect at low magnetic field H.

$$\varepsilon_{k_y,\sigma}(k) = -2t_{\|} \cos(k) - t_{\perp} \cos(k_y) - H\frac{\sigma}{2} \quad (2)$$

(with $k=k_x$ for simplicity and $k_y=0,\pi$) and is sketched in Fig. 1. If we denote by k^{σ}_{F,k_y} the Fermi wave vectors, we have the Luttinger sum rule

$$n = \frac{1}{2\pi} \sum_{(k_y,\sigma)\text{occ.}} k^{\sigma}_{F,k_y}, \quad (3)$$

where $n=N^e/(2L)=1-\delta$ is the electron density, δ the hole density, and L the length of the ladder. Experimentally, copper oxide systems have a fixed hole doping δ rather than a fixed chemical potential μ so δ will be kept fixed in this paper. Similarly, the magnetization per site $m=(N^{\uparrow}-N^{\downarrow})/(2L)$ satisfies

$$m = \frac{1}{2\pi} \sum_{(k_y,\sigma)\text{occ.}} \sigma k^{\sigma}_{F,k_y}. \quad (4)$$

Relations (3) and (4) are also valid in the presence of interactions. For quasi-one-dimensional interacting systems, a useful theorem is the generalization of the Lieb-Schultz-Mattis theorem to doped and magnetized states done by Yamanaka-Oshikawa-Affleck[29] (YOA). This theorem relates gap openings to commensurability conditions. When dealing with spinful fermions, the demonstration is based on the definition of two twist operators for spins $\uparrow$, $\downarrow$, which gives two commensurability conditions for parameters in each sector. In the case of doped two-leg ladders, YOA parameters take the simple form[26] $1-\delta+\sigma m$. If a parameter is a noninteger, the spectrum has gapless excitations in this sector. If a parameter is a noninteger but rational, a gap can open in the sector (*depending* on the relevance of interactions) but necessarily the ground state is degenerate with translational symmetry breaking. When the parameter is an integer, the sector is gapless or it is gapped but with a nondegenerate ground state. It is interesting to note that for $m,\delta\neq 0$, the sector $\uparrow$ can get gapped while the sector $\downarrow$ remains gapless (which corresponds to the $m=\delta$ plateau phase in Sec. IV) so that the usual spin-mode–charge-mode separation present when $m=0$ is no longer valid.

In the strong-coupling limit of the Hubbard model $U \gg t$ and for small hole doping, Hamiltonian (1) reduces to the *t-J* model:

$$\mathcal{H} = -t_{\parallel} \sum_{i,p=1,2,\sigma} \mathcal{P}[c^{\dagger}_{i+1,p,\sigma} c_{i,p,\sigma} + \text{H.c.}]\mathcal{P}$$
$$- t_{\perp} \sum_{i,\sigma} \mathcal{P}[c^{\dagger}_{i,2,\sigma} c_{i,1,\sigma} + \text{H.c.}]\mathcal{P}$$
$$+ J_{\parallel} \sum_{i,p=1,2} \left[\mathbf{S}_{i,p} \cdot \mathbf{S}_{i+1,p} - \frac{1}{4} n_{i,p} n_{i+1,p} \right]$$
$$+ J_{\perp} \sum_{i} \left[\mathbf{S}_{i,1} \cdot \mathbf{S}_{i,2} - \frac{1}{4} n_{i,1} n_{i,2} \right] - \sum_{i,p=1,2} H \cdot \mathbf{S}_{i,p}, \quad (5)$$

in which $\mathcal{P}$ is the Gutzwiller projector, $n_{i,p}=\Sigma_{\sigma} n_{i,p,\sigma}$, and the same convention is used to label the antiferromagnetic couplings $J_{\parallel,\perp}=4t^2_{\parallel,\perp}/U$. In what follows, these two microscopic models will be studied numerically and the isotropic model will assume $t=t_{\parallel}=t_{\perp}$ and $J=J_{\parallel}=J_{\perp}$.

Bosonization allows us to study the low-energy properties and correlation functions of one-dimensional-like systems using field theoretical methods. The bosonization Hamiltonians used to describe ladders[30–34] fall into two classes, coupled-band models to be reviewed in Sec. IV and coupled-chain models to be reviewed in Sec. V. The first approach is more appropriate to study the system with isotropic parameters. There is, however, the possibility, by strongly reducing the interchain hopping amplitude $t_{\perp}$, to obtain a crossover to a regime where the coupled-chain model is best suited to describe the behavior of the system (Sec. V).

III. NONINTERACTING AND STRONG-COUPLING LIMITS

Noninteracting system. It is interesting to discuss first the noninteracting system using relation (2) and keeping δ fixed instead of the chemical potential. Two main cases are possible: either a strong interband coupling with $t_{\perp}>2t_{\parallel}$ or a small interband coupling with $t_{\perp}<2t_{\parallel}$.

In the first case, the only bands which are partially filled at low magnetic field are the up- and down-spin bonding bands $(0,\uparrow)$ and $(0,\downarrow)$ [see Fig. 2(a)]. A first critical field corresponds to the complete filling of $(0,\uparrow)$ [Fig. 2(b)]. This induces a plateau with $m=\delta$ in the magnetization curve. This plateau is doping dependent and similar to what has been predicted for other doped systems.[12,13] The width of the plateau can be deduced from energetic considerations[13] to be $2(t_{\perp}-2t_{\parallel})$ in our case. When the plateau ends [Fig. 2(c)], the band $(\pi,\uparrow)$ starts to be partially filled. When the band $(0,\downarrow)$ gets empty, all electrons are polarized and the magnetization curve is constant with value $m=1-\delta$. For open boundary conditions (OBCs), a $m=\delta$ plateau is also found as displayed

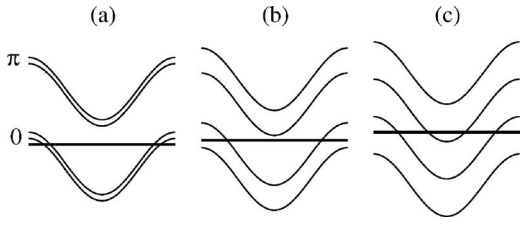

FIG. 2. Band evolution corresponding to Fig. 3.

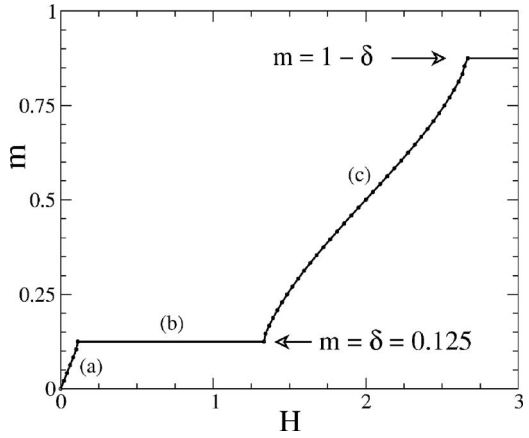

FIG. 3. Magnetization curves for the free system with $t_{\parallel}=0.2$ and $t_{\perp}=1.0$ showing a plateau at $m=\delta$ of width $2(t_{\perp}-2t_{\parallel})$.

in Fig. 3 (see Sec. IV E 1 for computational details). The width is in good agreement with $2(t_{\perp}-2t_{\parallel})$. Note that this plateau does not originate from interactions, contrary to what will be discussed in the strong-coupling approach below and in Sec. IV E 1, but is simply due to band-filling effects.

In the second case, all four bands are partially filled at low magnetic field. No plateaus are found but filling or emptying successively the bands will induce cusps in the magnetization curve and a decrease of the slope of the magnetization because fewer electrons contribute to the magnetization. First, the band $(\pi,\downarrow)$ gets empty, next, $(0,\uparrow)$ becomes completely filled, and lastly, $(0,\downarrow)$ gets empty corresponding to the saturation of the magnetization. An example of such a curve for $t_{\parallel}=t_{\perp}$ with OBC is given in Fig. 16. Two cusps are visible in this curve as well as a decrease of the average slope of the magnetization.

Qualitative remarks on the strong-coupling limit. Adding interactions in the system offers the possibility to study magnetization plateaus due to interactions and also pairing, which does not necessarily mean superconductivity. In this limit, we have $J_{\parallel},t_{\parallel},t_{\perp}\ll J_{\perp}$ and the pairing energy defined as in Eq. (33) is estimated to be[35] $J_{\perp}-2t_{\perp}-2t_{\parallel}$ and remains approximately constant under magnetic field because the average magnetization in Eq. (33) is zero. Two ground states are possible at finite magnetization: either holes are paired up and all the polarization is due to triplets, or hole pairs are split apart and the partner electron on the rung holds the polarization. The difference between the energies per rung of these two states is

$$m<\delta\text{: } \Delta e \sim (J_{\perp}-2t_{\perp}-2t_{\parallel})\delta - J_{\perp}m,$$

$$m>\delta\text{: } \Delta e \sim (2J_{\perp}-2t_{\perp}-2t_{\parallel})\delta - 2J_{\perp}m.$$

If $J_{\perp}/(t_{\perp}+t_{\parallel})>2$, a transition is then possible from the state with paired holes to the state with unpaired holes. The corresponding critical magnetization $m_c=[1-2(t_{\perp}+t_{\parallel})/J_{\perp}]\delta$ is always smaller than δ. This also gives a possible scenario for a wide $m=\delta$ plateau due to interactions. For large $J_{\perp}$ and $m=0$, we expect the ground state to have pairs of holes and singlets mostly on rungs so that the system has a large spin

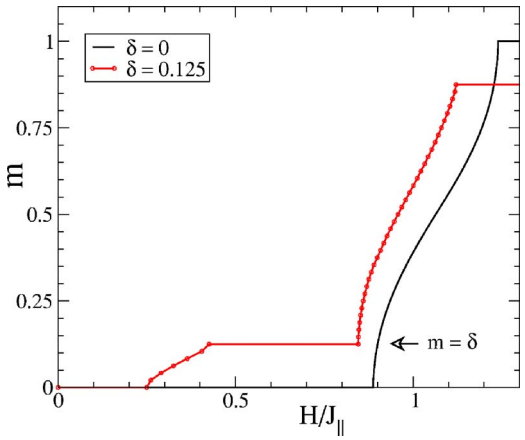

FIG. 4. (Color online) Plateaus in the strong-coupling limit. We chose $J_\perp=2.5$, $J_\parallel=0.3$, and $t_\parallel=t_\perp=1.0$. The $m=\delta$ plateau is an effect of interactions and the ground state in this plateau has unpaired holes. Still, holes are paired for magnetizations with $m \leqslant m_c < \delta$.

gap, which gives a $m=0$ plateau. However, the $m=0$ plateau is much smaller than the half-filling spin gap because polarized spins, in fact, gain kinetic energy if they are localized next to holes so that it is easier to create them. As the magnetic field is increased, hole pairs are split as suggested by the above argument and the partner electron of the hole on the rung becomes polarized. When all of them are fully polarized, we enter the $m=\delta$ plateau because the next spin excitation one can do is to flip a singlet on a rung, which cost is approximately $J_\perp$. The $m=\delta$ plateau can thus be wider than the $m=0$ one. This scenario corresponds to Fig. 4, where no pairing is found in the plateau from the computation of local densities of spins and holes with DMRG. Such a scenario could be relevant for compounds with lightly coupled dimers which could be doped with holes.

When one starts with unpaired holes at zero magnetic field, for instance, with $t_\parallel=J_\parallel \ll t_\perp=J_\perp$, the large half-filled spin gap of order $J_\perp-J_\parallel$ is immediately destroyed by doping (see Fig. 5). Increasing the magnetic field further quickly brings the system into a plateau phase with unpaired holes.

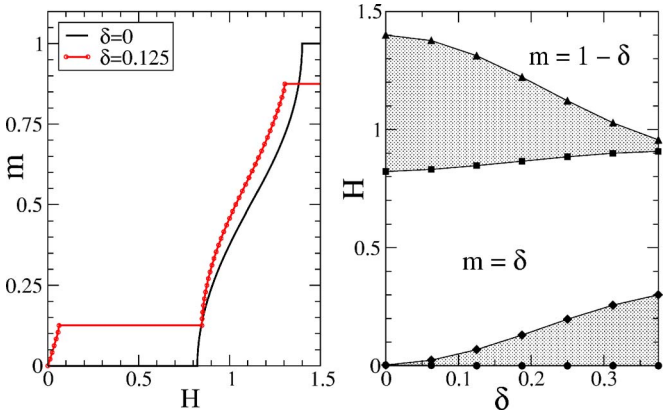

FIG. 5. (Color online) Plateau phase diagram of a two-leg ladder for $t_\perp=J_\perp=1.0$ and $t_\parallel=J_\parallel=0.2$. Doping immediately destroys the $m=0$ plateau present at half-filling, while a large doping-dependent $m=\delta$ plateau appears for a small critical field.

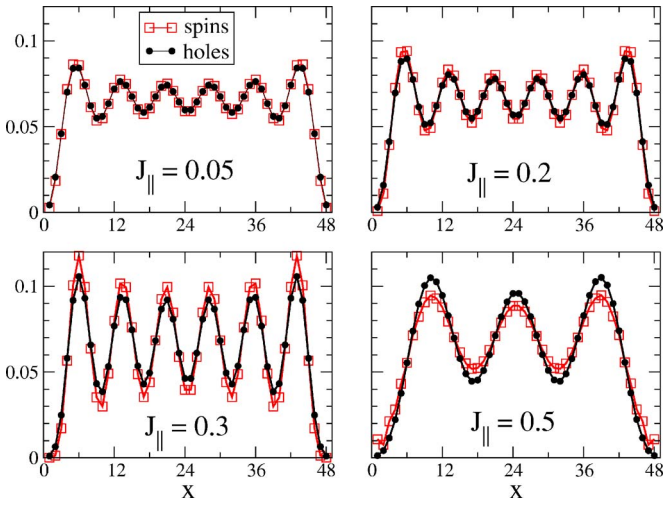

FIG. 6. (Color online) Local densities of holes and spins in the ground state of the $m=\delta$ phase computed on a ladder with $L=48$ and 6 holes, $t_\perp=t_\parallel=1.0$, and $J_\perp=0.5$. As $J_\parallel$ increases from 0 to $J_\parallel$ hole pairs form in the isotropic limit.

While the magnetization curve is similar to the noninteracting one below the $m=\delta$ plateau, its width is clearly controlled by $J_\perp-J_\parallel$ rather than by $2(t_\perp-2t_\parallel)$.

An interesting feature on the pairing of holes in the $m=\delta$ plateau is the occurrence of a transition when $J_\parallel$ is increased from 0 to $J_\perp$ from a state with unpaired holes to paired holes (see Fig. 6). Having pairing in this plateau is a situation that is not expected in the strong-coupling limit as we have seen, but for intermediate $J_\perp$, we expect that hopping between hole pairs and magnons can stabilize hole pairs[23] (see Sec. IV). Figure 6 suggests that a $J_\parallel$ comparable to $J_\perp$ is also needed to have pairing in this phase.

IV. COUPLED-BAND REGIME

A. Bosonized Hamiltonian

When the interactions are not too strong compared to the interchain hopping, it is reasonable to begin to solve the noninteracting band structure and then add interactions. This is the approach followed in Refs. 32–34. The noninteracting band structure is simply formed of the bonding band of energy $\varepsilon_{0,\sigma}(k)$ and an antibonding band of energy $\varepsilon_{\pi,\sigma}(k)$. The annihilation operators of the fermions in these bands are, respectively, given by

$$\psi_{0,\sigma}=\frac{1}{\sqrt{2}}(\psi_{1,\sigma}+\psi_{2,\sigma}), \quad \psi_{\pi,\sigma}=\frac{1}{\sqrt{2}}(\psi_{1,\sigma}-\psi_{2,\sigma}),$$

with 1 and 2 the labels of the chains. In the continuum limit, the fermions 0 and π are bosonized in terms of the boson fields $\phi_{k_y,\sigma}$ $(k_y=0,\pi)$ so that we write the fermion operator

$$c_{n,k_y,\sigma} \to \sqrt{a}\psi_{k_y,\sigma}(x)=\sqrt{a}[e^{ik^\sigma_{F,k_y}x}\psi_{R,k_y,\sigma}(x)+e^{-ik^\sigma_{F,k_y}x}\psi_{L,k_y,\sigma}(x)], \tag{6}$$

in which $x=na$ (a is the lattice spacing) and

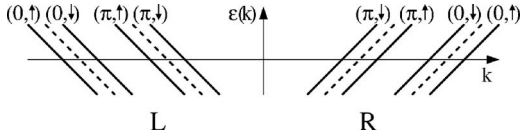

FIG. 7. Schematic representation of bosonized bands in the coupled-band models.

$$\psi_{R/L,k_y,\sigma} = \frac{\eta_{R/L,k_y,\sigma}}{\sqrt{2\pi\alpha}} e^{i\epsilon_{R/L}\phi_{R/L,k_y,\sigma}},$$

where R,L are the labels for the right and left movers (see Fig. 7), α is a cutoff (typically a), $\epsilon_{R/L}=\mp 1$, and η are Klein factors needed to make the annihilation operators of the different fermion species anticommute. We also have the definitions $\phi_{k_y,\sigma}=\frac{1}{2}[\phi_{L,k_y,\sigma}+\phi_{R,k_y,\sigma}]$, while dual fields are $\theta_{k_y,\sigma}=\frac{1}{2}[\phi_{L,k_y,\sigma}-\phi_{R,k_y,\sigma}]=\pi\int \Pi_{k_y,\sigma}$.

We then introduce the useful bosons ϕ_{ν,k_y} with $\nu=c,s$ for charge (spin) corresponding to the symmetric (antisymmetric) combination of $\phi_{k_y,\uparrow}$ and $\phi_{k_y,\downarrow}$. The same transformation is performed on the dual fields, leading to the Hamiltonian

$$\mathcal{H} = \sum_{\substack{k_y=0,\pi \\ \nu=c,s}} \int \frac{dx}{2\pi}[u_{k_y}(\pi\Pi_{\nu,k_y})^2 + u_{k_y}(\partial_x\phi_{\nu,k_y})^2],$$

where $[\phi_{\nu,k_y}(x),\Pi_{\nu',k_y'}(x')]=i\delta_{\nu,\nu'}\delta_{k_y,k_y'}\delta(x-x')$. In the following, we will make the usual approximation[36] of neglecting the difference between the velocities u_{k_y} of the 0 and π bands. This allows us to introduce the linear combinations

$$\phi_{c,\pm} = \frac{1}{\sqrt{2}}(\phi_{c,0} \pm \phi_{c,\pi}), \quad \phi_{s,\pm} = \frac{1}{\sqrt{2}}(\phi_{s,0} \pm \phi_{s,\pi}),$$

with similar definitions for the dual fields $\theta_{\nu,\pm}=\pi\int \Pi_{\nu,\pm}$. In the most general case, we have to use a Z matrix to describe the evolution of the system under magnetic field.[37] When comparing the results with the chain models of Sec. V, it is useful to note that while $\phi_{c+}=\phi_{\rho+}$ and $\phi_{s+}=\phi_{\sigma+}$ (we use Greek letters for the fields defined in the chain models and Latin letters for the fields defined in the band models), there is no simple relation between $\phi_{\rho-}$ and ϕ_{c-} and between ϕ_{s-} and $\phi_{\sigma-}$. The magnetic field couples to the system by a term

$$\mathcal{H} = \frac{H}{\pi}\int dx \partial_x\phi_{s+}. \tag{7}$$

Once interactions are turned on, two types of terms appear in the Hamiltonian. The terms of the first type are forward-scattering interaction terms that are quadratic in the fields $\phi_{\nu,\pm}$. The terms of the second type are backscattering interaction terms, the expressions of which were derived in Ref. 33. Since terms containing $\cos 2\phi_{s+}$ cannot appear in the Hamiltonian when the magnetization is nonzero, the expression of the backscattering terms in a magnetized ladder reads

$$\mathcal{H}_{\text{back}} = \int dx \cos 2\theta_{c-}\left[\frac{2g_A}{(2\pi\alpha)^2}\cos 2\phi_{s-} + \frac{2g_B}{(2\pi\alpha)^2}\cos 2\theta_{s-}\right]. \tag{8}$$

From the Hamiltonian (8), one sees that in the ground state the field θ_{c-} is pinned to $\langle\theta_{c-}\rangle=0$. By using the results of Ref. 38 [Sec. 3.1 and Eqs. (20) and (56)], one can argue that in the presence of repulsive interactions, one must have $K_{s-}<1$. Thus, one obtains a freezing of the field related to the most relevant operator $\langle\phi_{s-}\rangle=\frac{\pi}{2}$. Briefly, when $m=\delta=0$, all fields are massive and we have the famous spin-liquid phase, often denoted by C0S0. When $m=0$ but $\delta\neq 0$, the system with repulsive interactions is in a C1S0 phase, or Luther-Emery (LE) phase, with sectors $c-$ and $s\pm$ being massive while the sector $c+$ is massless, corresponding to the charge mode. When $m\neq 0$ and $\delta\neq 0$, the sector $s+$ becomes massless, giving rise to a C1S1 phase. Luttinger exponents associated with these sectors will be denoted by $K_{c/s+}$. Until now, we have discussed the case of generic nonzero magnetization. For the specific case $m=\delta$, however, a magnetization plateau can be expected. Following Ref. 26, we introduce the fields

$$\phi_\sigma^\pm = \frac{1}{\sqrt{2}}(\phi_{c,\pm} + \sigma\phi_{s,\pm}), \tag{9}$$

which appear in the term that induces the opening of the $m=\delta$ plateaus,

$$\int dx \cos[2(k_{F,0}^\sigma + k_{F,\pi}^\sigma)x - 2\sqrt{2}\phi_\sigma^+], \tag{10}$$

with, from Eqs. (3) and (4), the relation $k_{F,0}^\sigma + k_{F,\pi}^\sigma = \pi(n+\sigma m)$. This term leads to the opening of plateaus when $n\pm m\in\mathbb{Z}$ as expected in the YOA theorem. This condition is a commensurability condition which combines both spin and charge degrees of freedom. The $m=\delta$ plateau corresponds to the locking of the $\phi_\uparrow^+$ mode. The origin of term (10) giving rise to the plateau is the Hubbard interaction $Un_{i\uparrow}n_{i\downarrow}$ which contains the terms

$$(c_{0\uparrow}^\dagger c_{\pi\uparrow} + c_{\pi\uparrow}^\dagger c_{0\uparrow})(c_{0\downarrow}^\dagger c_{\pi\downarrow} + c_{\pi\downarrow}^\dagger c_{0\downarrow}), \tag{11}$$

which, once bosonized, yields Umklapp terms such as

$$\int dx \cos[2(k_{F,0}^\uparrow + k_{F,\pi}^\uparrow)x - 2(\phi_{0,\uparrow} + \phi_{\pi,\uparrow})]. \tag{12}$$

B. Superconducting order parameters and most divergent fluctuations

In this section, we define the order parameters for superconductivity at nonzero magnetization (high field), derive their bosonized expressions, and deduce their long-range correlations. Since the SU(2) symmetry is broken by the magnetic field, we have to compute the superconducting correlation functions $\langle\Delta_{\sigma\sigma'}^\lambda(x)\Delta_{\sigma\sigma'}^{\lambda\dagger}(0)\rangle$ in various channels λ. We use the following microscopic definitions for the pairing operators $\Delta_{\sigma\sigma'}^\lambda(n)$ at rung n:

$$\text{singlet: } \Delta^{s}_{\uparrow\downarrow}(n) = \sum_{\sigma} \sigma c_{r\sigma} c_{r'-\sigma}, \tag{13}$$

$$\text{triplet: } \begin{cases} \Delta^{t}_{\uparrow\downarrow}(n) = \sum_{\sigma} c_{r\sigma} c_{r'-\sigma} \\ \Delta^{t}_{\uparrow\uparrow}(n) = c_{r\uparrow} c_{r'\uparrow} \\ \Delta^{t}_{\downarrow\downarrow}(n) = c_{r\downarrow} c_{r'\downarrow}, \end{cases} \tag{14}$$

with $r=(n,1)$ and $r'=(n,2)$ for next-nearest-neighbor pairs created on a rung and $r=(n,p)$ and $r'=(n+1,p)$ if created on the leg p. Contrary to the case of the coupled-chain regime (Sec. V) where the Fermi wave vectors are the same in both chains, in the case of the band regime the Fermi wave vectors of the two bands are different ($k^{\sigma}_{F,0} \neq k^{\sigma}_{F,\pi}$) as can be seen in Fig. 1. As a result, a more detailed derivation of the bosonized expressions starting from lattice expressions in a two-chain Hubbard model becomes necessary.

1. Bosonized form

Using the bosonized form (6) of the fermion operators, we can express these order parameters as a function of products of the $\psi_{R/L,k_y,\sigma}$. In this section, only components with the dominant contribution will be kept, i.e., we will neglect terms of the form $\psi_R\psi_R$ and $\psi_L\psi_L$. These dominant contributions correspond to pairing with the lowest total momentum q. The case of $2k_F$ triplet pairing will be discussed in Sec. IV B 2. At finite magnetization, the equality of the velocities and Eq. (4) ensures that the lowest momentum is $q=k^{\uparrow}_{F,0/\pi} - k^{\downarrow}_{F,0/\pi} = \pi m$. To simplify the expression of the operators, we will use extensively the following results on a pinned field φ (for which $\langle\varphi\rangle$=cste): we can replace $\langle f(\varphi)\rangle$ by $f(\langle\varphi\rangle)$ and the dual field has exponentially decaying correlation functions.[39]

Starting with the interband order parameters, which read

$$\psi_{R,0,\sigma}\psi_{L,\pi,-\sigma} \sim e^{i[\theta_{c+}-\phi_{c-}-\sigma(\phi_{s+}-\theta_{s-})]},$$

$$\psi_{R,0,\sigma}\psi_{L,\pi,\sigma} \sim e^{i[\theta_{c+}-\phi_{c-}-\sigma(\theta_{s+}-\phi_{s-})]},$$

we note that they are all proportional to $e^{i\phi_{c-}}$ and thus, since θ_{c-} is pinned, their correlations decay exponentially. In other words, power-law decay is possible only for intraband superconducting correlations.

The intraband superconducting order parameters in the three spin channels read, respectively, as follows.

For intraband singlet,

$$\sum_{\sigma} \sigma\psi_{R,0,\sigma}\psi_{L,0,-\sigma} \sim \sum_{\sigma} \sigma e^{i[\theta_{c+}+\theta_{c-}-\sigma(\phi_{s+}+\phi_{s-})]},$$

$$\sum_{\sigma} \sigma\psi_{R,\pi,\sigma}\psi_{L,\pi,-\sigma} \sim \sum_{\sigma} \sigma e^{i[\theta_{c+}-\theta_{c-}-\sigma(\phi_{s+}+\phi_{s-})]}.$$

For intraband triplet $S^z=0$,

$$\sum_{\sigma} \psi_{R,0,\sigma}\psi_{L,0,-\sigma} \sim \sum_{\sigma} e^{i[\theta_{c+}+\theta_{c-}-\sigma(\phi_{s+}+\phi_{s-})]},$$

$$\sum_{\sigma} \psi_{R,\pi,\sigma}\psi_{L,\pi,-\sigma} \sim \sum_{\sigma} e^{i[\theta_{c+}-\theta_{c-}-\sigma(\phi_{s+}-\phi_{s-})]}.$$

For intraband triplet $S^z=1$,

$$\psi_{R,0,\sigma}\psi_{L,0,\sigma} \sim e^{i[\theta_{c+}+\theta_{c-}+\sigma(\theta_{s+}+\theta_{s-})]},$$

$$\psi_{R,\pi,\sigma}\psi_{L,\pi,\sigma} \sim e^{i[\theta_{c+}-\theta_{c-}+\sigma(\theta_{s+}-\theta_{s-})]}.$$

To determine which forms of superconductivity will be dominant, we need to express the leg and rung order parameters in terms of the intraband order parameters. We have for the rung singlet order parameter

$$\Delta^{s}_{\uparrow\downarrow}(x) \sim \sum_{\sigma} \frac{\sigma}{2} e^{i\sigma qx}(\psi_{R,0,\sigma}\psi_{L,0,-\sigma} - \psi_{R,\pi,\sigma}\psi_{L,\pi,-\sigma}), \tag{15}$$

whereas the rung triplet $S^z=0$ is given by

$$\Delta^{t}_{\uparrow\downarrow}(x) \sim \sum_{\sigma} \frac{1}{2} e^{i\sigma qx}(\psi_{R,\pi,\sigma}\psi_{L,0,-\sigma} - \psi_{R,0,-\sigma}\psi_{L,\pi,\sigma}). \tag{16}$$

Therefore, since it is composed only of interband terms, we expect that its correlation will present exponential decay. Lastly, for the rung triplet $S^z=1$ order parameter, we find

$$\Delta^{t}_{\uparrow\uparrow}(x) \sim \frac{1}{2}(\psi_{R,0,\uparrow}\psi_{L,0,\uparrow} - \psi_{R,\pi,\uparrow}\psi_{L,\pi,\uparrow}). \tag{17}$$

Turning to the leg singlet order parameter, we find that it reads

$$\Delta^{s}_{\uparrow\downarrow}(x) \sim \sum_{\sigma} \frac{\sigma}{2} e^{i\sigma qx}[e^{-ik^{-\sigma}_{F,0}a}\psi_{R,0,\sigma}\psi_{L,0,-\sigma} + (0 \to \pi)]. \tag{18}$$

Note that because we can neglect interband coupling, the expression is the same on both legs. Thus, leg-leg correlations on the same leg and between the legs will have the same sign as found numerically in Fig. 8. Analogously, the leg triplet $S^z=0$ operator reads

$$\Delta^{t}_{\uparrow\downarrow}(x) \sim \sum_{\sigma} \frac{1}{2} e^{i\sigma qx}[\sin(k^{\sigma}_{F,0}a)\psi_{R,0,\sigma}\psi_{L,0,-\sigma} + (0 \to \pi)]. \tag{19}$$

Note that if we take the limit $a \to 0$, this term disappears as happened for the rung triplet. Finally, the leg triplet $S^z=1$ reads

$$\Delta^{t}_{\uparrow\uparrow}(x) \sim \frac{1}{2}[e^{-ik^{\uparrow}_{F,0}a}\psi_{R,0,\uparrow}\psi_{L,0,\uparrow} + (0 \to \pi)]. \tag{20}$$

Since $K_{s-} < 1$, we have $\langle\phi_{s-}\rangle = \frac{\pi}{2}$. Then, all the intraband triplets $S^z=1$ have exponentially decaying correlations. As a consequence, both the leg and the rung triplets with $S^z=1$ have exponentially decaying correlations. The behavior of these correlations with higher $2k_F$ momentum will be discussed in Sec. IV B 2. Another consequence of the ordering of the field ϕ_{s-} is that

$$\psi_{R,0,\sigma}\psi_{L,0,-\sigma} \sim e^{-i(\pi/2)\sigma} e^{i(\theta_{c+}-\sigma\phi_{s+})},$$

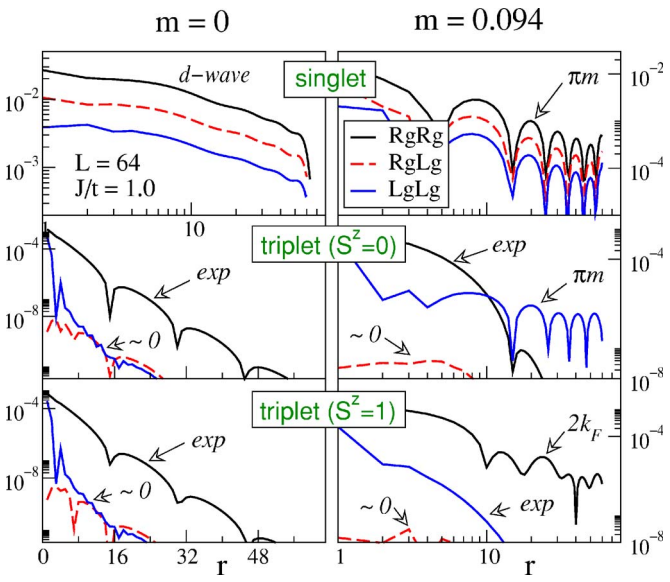

FIG. 8. (Color online) Absolute value of superconducting correlations for zero and a finite magnetization in an isotropic doped ladder with δ=0.063. Notations are "Rg" for rung, "Lg" for leg, "~0" for numerically irrelevant signal, "*exp*" for exponentially decaying correlations, and "πm" and "$2k_F$" for the wave vectors. Note that the S^z=1 "$2k_F$" oscillations are smoothed out by taking the absolute value. M=1000 states were kept with discarded weight of order 10^{-6}.

$$\psi_{R,\pi,\sigma}\psi_{L,\pi,-\sigma} \sim e^{i(\pi/2)\sigma}e^{i(\theta_{c+}-\sigma\phi_{s+})}.$$

Provided that $k_{F,0} \neq k_{F,\pi}$, the leg triplet S^z=0 order parameter does not vanish. We find that it has the same critical exponent as the rung singlet order parameter, namely, $\frac{1}{2}(K_{c+}^{-1}+K_{s+})$. It is larger than the m=0 critical exponent $1/(2K_{c+})$ because of the appearance of the massless boson θ_{s+}. The fact that we have a finite momentum pairing with $q=\pi m$ is very likely to occur in a one-dimensional-like system and is the signature of the FFLO mechanism.

2. S^z=1 triplet with a $2k_F$ momentum

Another notable result is the presence of rung-rung triplet S^z=1 correlations with $2k_F$ oscillations. Within the band representation, it is indeed possible to find a component of the rung-rung triplet correlations that has power-law decay. Let us consider the next terms in the expansion of the rung triplet operator:

$$\psi_{1,\sigma}\psi_{2,\sigma} \sim -2e^{i(k_{F,0}^{\sigma}+k_{F,\pi}^{\sigma})x}\psi_{R,0,\sigma}\psi_{R,\pi,\sigma} + \cdots .$$

In bosonized form, this operator reads

$$\Delta_{\sigma\sigma,2k_F}^{t}(x) \sim e^{i(k_{F,0}^{\sigma}+k_{F,\pi}^{\sigma})x}e^{i[\theta_{c+}-\phi_{c+}+\sigma(\theta_{s+}-\phi_{s+})]}.$$

It has power-law correlations with a critical exponent

$$\frac{1}{2}(K_{c+}+K_{c+}^{-1}+K_{s+}+K_{s+}^{-1}),$$

and from Eqs. (3) and (4), the associated wave vector is $k_{F,0}^{\sigma}+k_{F,\pi}^{\sigma}=\pi(n+\sigma m)$. Note that its critical exponent is always larger than the one of the rung singlet order parameter.

3. Charge-density wave order parameters

Here, we address the question of the CDW exponents under magnetic field. First, the $2k_F$ CDW order parameter n_i, which vanishes exponentially at zero magnetization, contains terms such as

$$\psi_{r,0\sigma}^{\dagger}\psi_{r,\pi\sigma} \sim e^{i[\phi_{c-}+\sigma\phi_{s-}-r(\theta_{c-}+\sigma\theta_{s-})]},$$

with $r=\pm$ for R,L and a wave vector $k_{F,\pi}^{\sigma}-k_{F,0}^{\sigma}$. These order parameters decay exponentially because they are proportional to $e^{i\phi_{c-}}$. A last possible term is

$$\psi_{R,0\sigma}^{\dagger}\psi_{L,\pi\sigma} \sim e^{i[\phi_{c+}-\theta_{c-}+\sigma(\phi_{s+}-\theta_{s-})]},$$

with a "$2k_F$" wave vector $\pi(n+\sigma m)$. It decays exponentially because of $e^{i\theta_{s-}}$. Finally, no $2k_F$ CDWs are expected under magnetic field.

Secondly, the $4k_F$ CDW order parameter[16] is n_i^2 and has an exponent $2K_{c+}$ at zero magnetization. This order parameter contains terms such as

$$\psi_{R,0\sigma}^{\dagger}\psi_{L,0\sigma}\psi_{R,\pi\sigma}^{\dagger}\psi_{L,\pi\sigma} \sim e^{i2[\phi_{c+}+\sigma\phi_{s+}]},$$

which have a "$4k_F$" wave vector $2\pi(n+m)$ and, for nonzero magnetization, an exponent $2(K_{c+}+K_{s+})$. We also have terms like

$$\psi_{R,0\sigma}^{\dagger}\psi_{L,0\sigma}\psi_{R,\pi-\sigma}^{\dagger}\psi_{L,\pi-\sigma} \sim e^{i2[\phi_{c+}+\sigma\phi_{s-}]},$$

with a wave vector $2(k_{F,0}^{\sigma}+k_{F,\pi}^{-\sigma})$ and an exponent $2K_{c+}$ which is not affected by the magnetic field. This last term can compete with the superconducting order parameter to be the most diverging fluctuations depending on K_{c+} and K_{s+}.

C. Interpreting the superconducting critical field H_c as a band-filling transition

In this section, we identify the observed superconducting upper critical field H_c with a band-filling transition. Such a transition will ungap all three remaining sectors, leading to an enhancement of the correlation exponents. We describe the system just above the transition and compute the various possible exponents using bosonization. We consider a case where the Fermi energy is positioned in such a way that the band $(\pi,\downarrow)$ is empty while the three other bands remain partially filled (see Fig. 1 for illustration). The band $(\pi,\downarrow)$ being empty has important consequences. Projecting out the high-energy subspace where the band $(0,\downarrow)$ is occupied by a single electron, one gets in lowest order

$$c_{n,p,\downarrow}^{\dagger}c_{n,p,\downarrow} \rightarrow \frac{1}{2}c_{n,0,\downarrow}^{\dagger}c_{n,0,\downarrow}, \tag{21}$$

and as a result the on-site Hubbard interaction reduces to

$$\frac{U}{2}\sum_{n} n_{i,0,\downarrow}(n_{i,0,\uparrow}+n_{i,\pi,\uparrow}). \tag{22}$$

In the absence of commensuration between the different

TABLE I. The superconducting operators for the Hubbard model with an empty band corresponding to the coupled-band regime just above H_c.

Type of operator	Fermion expression	Dimension	Wave vector
$S^z=1$ triplet	$\psi_{R0\uparrow}\psi_{L0\uparrow}$	$\frac{1}{4K_1}+\frac{1}{4K_2}+\frac{1}{2K_3}$	0
	$\psi_{R\pi\uparrow}\psi_{L\pi\uparrow}$	$\frac{1}{4K_1}+\frac{1}{4K_2}+\frac{1}{2K_3}$	0
	$\psi_{R0\downarrow}\psi_{L0\downarrow}$	$\frac{1}{2K_1}+\frac{1}{2K_2}$	0
	$\psi_{R\pi\uparrow}\psi_{L0\uparrow}$	$\frac{1}{4K_1}+\frac{1}{4K_2}+\frac{K_3}{2}$	$k^{\uparrow}_{F\pi}-k^{\uparrow}_{F0}$
$S^z=0$ triplet or singlet	$\psi_{R0\uparrow}\psi_{L0\downarrow}$	$\frac{3+\sqrt{8}}{16}(K_1^{-1}+K_2)+\frac{3-\sqrt{8}}{16}(K_2^{-1}+K_1)+\frac{1}{8}(K_3+K_3^{-1})$	$k^{\uparrow}_{F0}-k^{\downarrow}_{F0}$
	$\psi_{R\pi\uparrow}\psi_{L0\downarrow}$	$\frac{3+\sqrt{8}}{16}(K_1^{-1}+K_2)+\frac{3-\sqrt{8}}{16}(K_2^{-1}+K_1)+\frac{1}{8}(K_3+K_3^{-1})$	$k^{\uparrow}_{F\pi}-k^{\downarrow}_{F0}$

bands, the resulting bosonized Hamiltonian has only forward-scattering interactions. Thus, its excitations are completely gapless. The bosonized Hamiltonian reads

$$\mathcal{H}=\mathcal{H}_0+\mathcal{H}_U,$$

$$\mathcal{H}_0=\sum_{\nu\in\{(0,\uparrow),(0,\downarrow),(\pi,\uparrow)\}}\int\frac{dx}{2\pi}v_{F,\nu}[(\pi\Pi_\nu)^2+(\partial_x\phi_\nu)^2], \tag{23}$$

$$\mathcal{H}_U=\frac{U\alpha}{2\pi^2}\int dx\partial_x\phi_{0,\downarrow}(\partial_x\phi_{0,\uparrow}+\partial_x\phi_{\pi,\uparrow}). \tag{24}$$

This Hamiltonian can be fully diagonalized. In the general case, where the Fermi velocities are all different, one needs to first perform a rescaling ($\Pi_\nu\rightarrow\sqrt{u/v_{F,\nu}}\Pi_\nu$ and $\phi_\nu\rightarrow\phi_\nu/\sqrt{u/v_{F,\nu}}$, where u is an arbitrary quantity with the dimension of a velocity) and then diagonalize the matrix

$$\begin{pmatrix} v_{F,0\uparrow}^2 & \frac{U\alpha}{4\pi^2}\sqrt{v_{F,0\uparrow}v_{F,0\downarrow}} & 0 \\ \frac{U\alpha}{4\pi^2}\sqrt{v_{F,0\uparrow}v_{F,0\downarrow}} & v_{F,0\downarrow}^2 & \frac{U\alpha}{4\pi^2}\sqrt{v_{F,\pi\uparrow}v_{F,0\downarrow}} \\ 0 & \frac{U\alpha}{4\pi^2}\sqrt{v_{F,0\uparrow}v_{F,0\downarrow}} & v_{F,\pi\uparrow}^2 \end{pmatrix}. \tag{25}$$

Afterward, one performs the inverse rescaling on the diagonal matrix to obtain the velocities of the modes and the associated Luttinger exponents. To simplify the algebra, we will assume that all the Fermi velocities are equal. Then, we find that the following combination of fields

$$\begin{pmatrix}\phi_1\\ \phi_2\\ \phi_3\end{pmatrix}=\begin{pmatrix}\frac{\sqrt{2}}{2} & \frac{1}{2} & \frac{1}{2}\\ \frac{\sqrt{2}}{2} & -\frac{1}{2} & -\frac{1}{2}\\ 0 & \frac{\sqrt{2}}{2} & -\frac{\sqrt{2}}{2}\end{pmatrix}\begin{pmatrix}\phi_{0,\downarrow}\\ \phi_{0\uparrow}\\ \phi_{\pi\uparrow}\end{pmatrix} \tag{26}$$

diagonalizes the interaction and

$$u_1K_1=u_2K_2=u_3K_3=v_F, \tag{27}$$

$$\frac{u_1}{K_1}=v_F+\frac{U\alpha}{2\pi^2\sqrt{2}}, \tag{28}$$

$$\frac{u_2}{K_2}=v_F-\frac{U\alpha}{2\pi^2\sqrt{2}}, \tag{29}$$

$$\frac{u_3}{K_3}=v_F. \tag{30}$$

In terms of these new fields, the fermion operators read

$$\psi_{r,0,\uparrow}=\frac{\eta_{r,0,\uparrow}}{\sqrt{2\pi\alpha}}e^{i[(1/2)(\theta_1-r\phi_1)-(1/2)(\theta_2-r\phi_2)+(1/\sqrt{2})(\theta_3-r\phi_3)]},$$

$$\psi_{r,\pi,\uparrow}=\frac{\eta_{r,\pi,\uparrow}}{\sqrt{2\pi\alpha}}e^{i[(1/2)(\theta_1-r\phi_1)-(1/2)(\theta_2-r\phi_2)-(1/\sqrt{2})(\theta_3-r\phi_3)]},$$

$$\psi_{r,0,\uparrow}=\frac{\eta_{r,0,\downarrow}}{\sqrt{2\pi\alpha}}e^{i(\sqrt{2}/2)[(\theta_1-r\phi_1)+(\theta_2-r\phi_2)]}.$$

From these expressions, it is possible to obtain the various superconducting order parameters and their critical exponents. The results are gathered in Tables I and II on which one must note that the correlation exponent will be twice the dimension of the operator.

TABLE II. The CDW/SDW operators for the Hubbard model with an empty band corresponding to the coupled-band regime just above H_c.

Type of operator	Fermion expression	Dimension	Wave vector
SDW^z/CDW	$\psi^\dagger_{R0\uparrow}\psi_{L0\uparrow}$	$\frac{K_1}{4}+\frac{K_2}{4}+\frac{K_3}{2}$	$2k^\uparrow_{F0}$
	$\psi^\dagger_{R\pi\uparrow}\psi_{L\pi\uparrow}$	$\frac{K_1}{4}+\frac{K_2}{4}+\frac{K_3}{2}$	$2k^\uparrow_{F\pi}$
	$\psi^\dagger_{R0\downarrow}\psi_{L0\downarrow}$	$\frac{K_1}{2}+\frac{K_2}{2}$	$2k^\downarrow_{F0}$
	$\psi^\dagger_{R\pi\uparrow}\psi_{L0\uparrow}$	$\frac{K_1}{4}+\frac{K_2}{4}+\frac{1}{2K_3}$	$k^\uparrow_{F\pi}+k^\uparrow_{F0}$
SDW^{x,y}	$\psi^\dagger_{R0\uparrow}\psi_{L0\downarrow}$	$\frac{3-\sqrt{8}}{16}(K_1^{-1}+K_2)+\frac{3+\sqrt{8}}{16}(K_2^{-1}+K_1)+\frac{1}{8}(K_3+K_3^{-1})$	$k^\uparrow_{F0}+k^\downarrow_{F0}$
	$\psi^\dagger_{R\pi\uparrow}\psi_{L0\downarrow}$	$\frac{3-\sqrt{8}}{16}(K_1^{-1}+K_2)+\frac{3+\sqrt{8}}{16}(K_2^{-1}+K_1)+\frac{1}{8}(K_3+K_3^{-1})$	$k^\uparrow_{F\pi}+k^\downarrow_{F0}$

D. Numerical results on superconducting correlation functions

We have computed superconducting correlation functions with DMRG using the definitions of Eqs. (13) and (14). As predicted by bosonization results, only modified d-wave singlet superconductivity is found when $m=0$ (rung-leg correlations have an opposite sign to rung-rung and leg-leg correlations, see Ref. 16 for a bosonization discussion), while $S^z=0$ leg-leg triplet and $S^z=1$ rung-rung triplet correlations emerge under high magnetic field (see Fig. 8 for the t-J model and Fig. 9 for the repulsive Hubbard model). Furthermore, these correlations oscillate with wave vectors $q=\pi m$ for the $S^z=0$ channel and $q=2k_F$ for the $S^z=1$ channel. The $q=\pi m$ relation has been checked in all the FFLO phases (see Fig. 17 and discussion in Sec. IV E) by fitting the oscillating correlations with $A\cos(qr+\varphi)/r^\alpha$ (see Fig. 10), confirming the FFLO-like mechanism. We observe that $S^z=0$ rung-rung triplet correlations have an exponential behavior, while rung-rung singlet correlations are algebraic, in agreement with the prediction from bosonization. Since from the point of view of the rotation symmetry these two order parameters transform in the same way, the difference must be caused by their different transformation properties under interchange of the legs. Note that because of the $\sin(k^\sigma_{F,k_y}a)$ factors in the leg singlet and $S^z=0$ leg triplet, the cancellation of the intraband terms obtained in the case of rung order parameters is absent. This explains the observation of power-law correlations. Concerning the orbital part of pairs, singlet Cooper pairs have a mixed s-wave and d-wave structure and $S^z=0$ triplet can be considered to first approximation as p-wave pairs along the legs (with a symmetric superposition of the two legs).

The good agreement with bosonization predictions relies on the fact that in the doped isotropic t-J ladder, four Fermi points exist with approximately[35] $k_{F,0}\sim 3\pi/5$ and $k_{F,\pi}\sim 2\pi/5$ when $m=0$ and that the assumption of equal Fermi

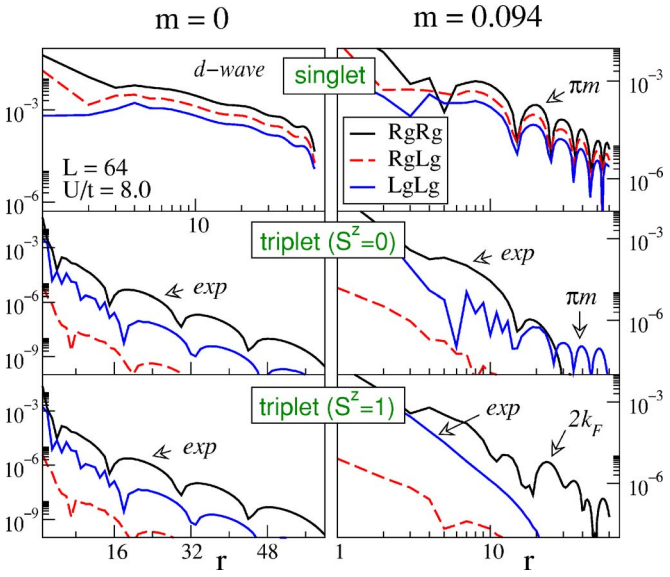

FIG. 9. (Color online) Same correlations as Fig. 8 but using the Hubbard model with $\delta=0.063$ and $U/t=8.0$. $M=1600$ states were kept with discarded weight of order 10^{-6}.

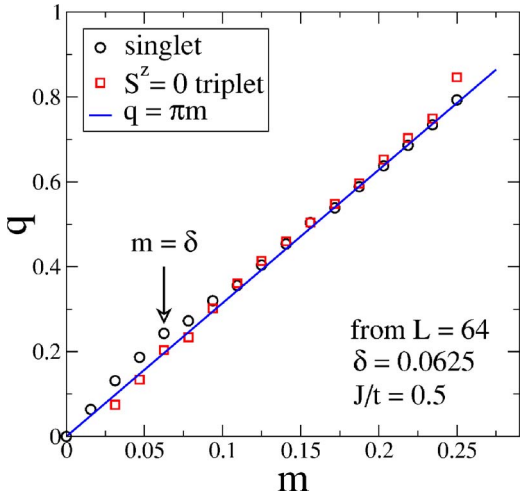

FIG. 10. (Color online) Verification of the $q=\pi m$ relation of FFLO-like pairing at finite magnetization in an isotropic ladder with $J/t=0.5$.

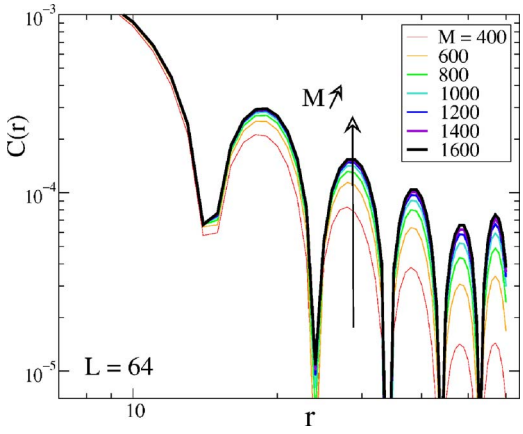

FIG. 11. (Color online) Convergence with the number of kept states M for a fixed length $L=64$. The plotted superconducting correlation is the singlet one and parameters are $m=0.094$, $\delta=0.063$, and $J/t=0.5$ which corresponds to the phase above the $m=\delta$ plateau and below the superconducting upper critical field H_c.

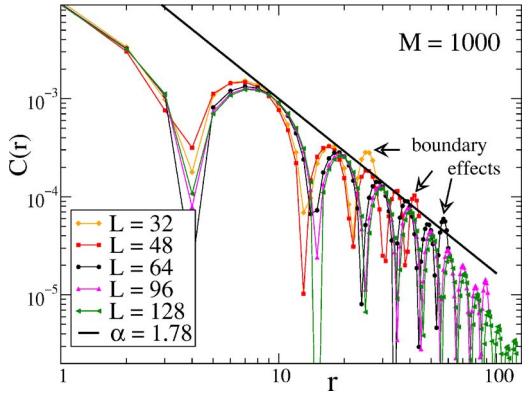

FIG. 12. (Color online) Convergence with size L for the same parameters as in Fig. 11, M being fixed.

velocities is numerically reasonable at low hole doping. The existence of a small leg-leg triplet component (about 100 times smaller than the rung-rung triplet) in the two-leg t-J ladder considered may therefore be explained by the persistence of a small band splitting in this strongly coupled ladder system.

We now would like to compare precisely the algebraic decay exponents α^s and α^t of the singlet and $S^z=0$ leg-leg triplet correlations. DMRG is known to often underestimate correlation functions[25] for a fixed number of kept states M. In order to capture the behavior in the thermodynamic limit, we computed the correlation functions for fixed M ranging from 800 to 2000 and lengths $L=32$, 64, 96, and 128 (we worked at fixed $\delta=1/16$ and $m=3/32$ so that these are the only accessible cluster sizes). We extracted $\alpha(M,L)$ by fitting the data. Then, we can extrapolate α in the $M\to\infty$ limit to get a correct exponent $\alpha(L)$ at size L from which we can do a finite-size scaling. In Fig. 11, we see that for a given size, $\alpha(M)$ decreases as M is enlarged, roughly like $\alpha(M)\sim 1/M$ [see Fig. 13(b)] as was previously found. We note from Fig. 12 that the larger the system, the larger M is needed to reach a good convergence. Convergence as a function of the discarded weight is also given in Fig. 13 and has qualitatively the same behavior. For $L=128$, the convergence is slower with M than for $L=96$, probably because we would need larger M to have a correct accuracy (the $1/M$ might be realized for large enough M) so that we believe the results are not as reliable as for $L=64$ and 96 (larger M would be very expensive numerically). On one side of Fig. 13(c), $M=2000$ is too small (for $L=128$), while on the other side, it is difficult to extract α because the system is too small to resolve enough oscillations (when $L=32$). Extrapolations can be tentatively done with some uncertainties which can be roughly estimated. Therefore, we can infer from Fig. 13 that $\alpha^s=1.54\pm0.15$ is greater than $\alpha^t=1.17\pm0.15$, which pleads in favor of dominating $S^z=0$ triplet correlations in this part of

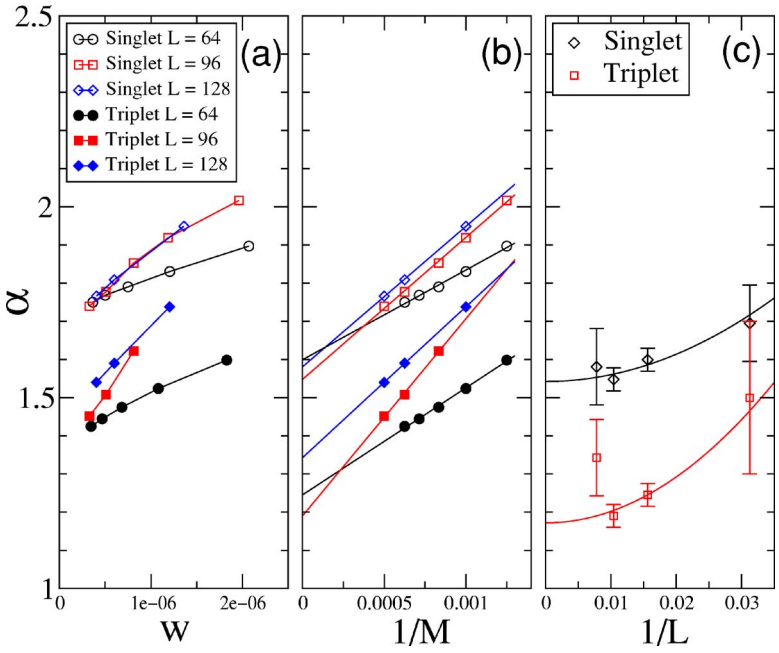

FIG. 13. (Color online) Extrapolation (a) of fitted exponent as a function of discarded weight w and (b) of the inverse of the number of kept states M for different lengths L. Extrapolated results from (b) are tentatively extrapolated vs L in (c). Large error bars occur when L is too small (for $L=32$) and because M is too small (for $L=128$). Parameters are given in the caption of Fig. 11.

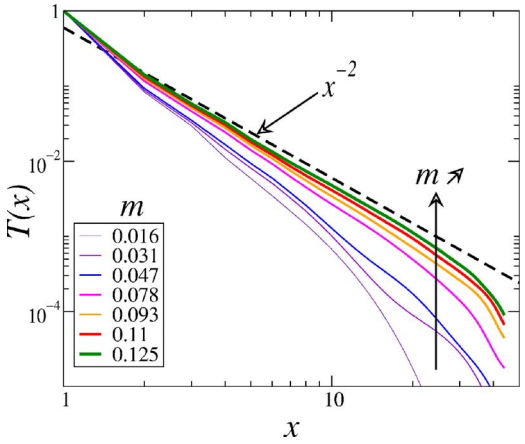

FIG. 14. (Color online) Normalized four-point spin correlations $T(x)=\langle S_2^+(x)S_1^+(x)S_2^-(0)S_1^-(0)\rangle$ for various magnetizations in the isotropic t-J ladder with $J/t=0.75$ and $\delta=0.063$. Their decay exponent is $2K_{s+}^{-1}$ which gives access to $K_{s+}(H)$. Correlations were computed on a system with $L=64$ and $M=1200$ states kept.

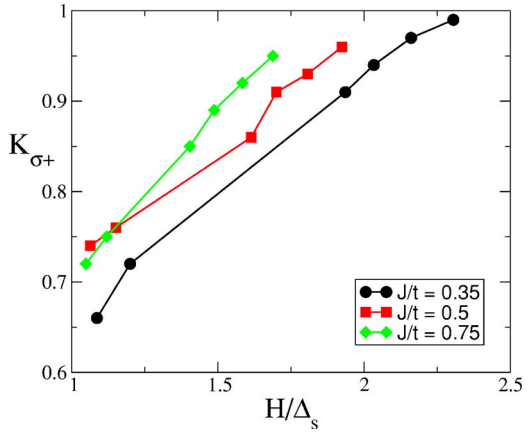

FIG. 15. (Color online) $K_{s+}(H/\Delta_s)$ from DMRG computations on a system with parameters of Fig. 14.

the phase diagram (above the $m=\delta$ plateau and below H_c) but the difference is rather small. Finite-size effects could explain that the bosonization prediction $\alpha^t=\alpha^s$ is not realized on numerical results. Note that $\alpha<2$ is sufficient to have a divergent superconducting susceptibility in the system. Concerning CDW exponents, they are difficult to compute numerically because of OBC but we will see that we can deduce from the two-particle gap of Fig. 18 that the system is in a superconducting phase.

1. Evolution of the Luttinger parameter K_{s+}

We now want to have access to the evolution of the Luttinger exponent K_{s+} of the gapless mode which appears at finite magnetization. We remark that the bosonized form of the triplet creation operator on a rung $S_2^+(x)S_1^+(x)$ contains dominant terms such as

$$\psi_{L,0\uparrow}^\dagger \psi_{L,0\downarrow} \psi_{R,\pi\uparrow}^\dagger \psi_{R,\pi\downarrow} \sim e^{-i2[\phi_{s-}+\theta_{s+}]}, \tag{31}$$

giving an exponent $2K_{s+}^{-1}$ since $\langle\phi_{s-}\rangle=\pi/2$. The wave vector associated with this operator is $(k_{F,0}^{\uparrow}-k_{F,0}^{\downarrow})-(k_{F,\pi}^{\uparrow}-k_{F,\pi}^{\downarrow})\sim 0$ since, if the difference between the Fermi velocities of the 0 and π bands is negligible, we have $k_{F,k_y}^{\uparrow}-k_{F,k_y}^{\downarrow}=\pi m$. Note that $2K_{s+}^{-1}$ is the smaller exponent for terms with this wave vector. Because $K_{s+}<1$, we could expect smaller possible exponents such as $2K_{s+}$ or $\frac{1}{2}[K_{s+}+K_{s+}^{-1}]$. For the first, one can show that fields $2[\phi_{s+}\pm\phi_{s-}]$ or $2[\phi_{s+}+\sigma\theta_{c-}]$ cannot appear in the decomposition of $S_2^+S_1^+$. For the other, fields $\phi_{s+}\pm\theta_{s+}\pm\theta_{c-}\pm\phi_{s-}$ cannot be decomposed in terms of the right and left mover fields with factors $\pm$. Finally, the decay exponent of the correlations of this order parameter is expected to be $2K_{s+}^{-1}$ and depends only on K_{s+} and not on K_{c+}. Numerically, we have computed the correlation function $\langle S_2^+(x)S_1^+(x)S_2^-(0)S_1^-(0)\rangle$. Data for the isotropic t-J model are displayed in Fig. 14 and show a power-law decay with an exponent larger than 2 and a wave vector approaching zero. Points are given as a function of H/Δ_s, Δ_s being the finite-size spin gap of the system. We thus have access to the evolution of K_{s+} as a function of the magnetic field (see Fig. 15). The general behavior is that $K_{s+}<1$ and increases with magnetic field toward the limit $K_{s+}=1$ at high fields. Similarly, the Luttinger parameter K_{s+} has been characterized using Bethe ansatz in the context of the SO(8) description of two-leg half-filled Hubbard ladders[40] which gave $K_{s+}<1$. When doped, the SO(6) description[41] gives the same constraint (results not shown) as well as an increase of K_{s+} at high magnetic field. However, a detailed comparison of SO(6) predictions and numerics would require one to determine first the conditions and parameters at which both approaches match and this is beyond the scope of this paper. Lastly, the values of K_{s+} obtained numerically should be slightly larger in the thermodynamic limit than what is found because of finite-size and finite M effects as explained above.

E. Generic phase diagram of the t-J model

In this section, we discuss the generic phase diagram in the (H,δ) plane for the isotropic t-J model on the basis of DMRG and bosonization results.

1. Doping-dependent magnetization plateaus

The magnetization curves $m(H)$ of Fig. 16, obtained within the Hubbard and t-J models, display plateaus for $m=0$ and $m=\delta$. Energies $E(n_h,S^z)$ were computed keeping $M=1600$ states with the single-site method proposed by White[42] (we used a noise level of 10^{-6}) at fixed hole number n_h and total magnetization S^z. Magnetic fields are deduced using $H(S^z)=E(n_h,S^z+1)-E(n_h,S^z)$, and interpolated with $[H(S^z)+H(S^z-1)]/2$ if they do not belong to a plateau. The $m=0$ plateau simply corresponds to the well-known spin gap of the doped ladder. The $m=\delta$ plateau exists at small doping for continuous values of δ (see Fig. 17 and Ref. 23) and thus falls into the classes of doping-dependent irrational magnetization plateaus predicted[12,26] by Cabra *et al.* It can be understood as a commensurate-incommensurate[43] (C-IC) transition so that we expect the critical exponent of the magnetization as a function of the magnetic field to be 1/2. In the plateau phase, the mode $\phi_\uparrow^+$ is locked but the sector $(\downarrow,+)$ remains gapless, leading to a metallic phase. Note that

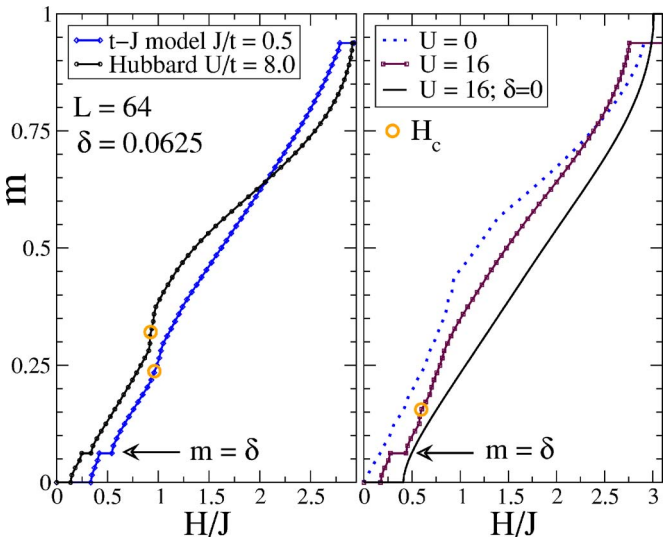

FIG. 16. (Color online) Magnetization curves for the isotropic *t-J*, Hubbard, and noninteracting systems. Irrational plateaus are clearly visible at $m=\delta$. H_c represents the superconducting critical field. The energy scale J is defined as $4t^2/U$ in the Hubbard model. The noninteracting system curve has been rescaled ($H \rightarrow H/4$) for clarity.

$\phi_{\uparrow}^{+}$ is a superposition of both spin and charge modes so that charge and spin are no more independent modes in the plateau phase.

The Hubbard and *t-J* models give qualitatively the same behavior at low magnetization. The spin gap ($m=0$ plateau) in the Hubbard model with $U/t=8$ is about half of the spin gap of the *t-J* model with $J/t=0.5$ as it was previously found,[44] but the irrational plateau has roughly the same width. A larger U gives a slightly larger plateau. Both models display a singularity of the magnetization curve, more or less pronounced, near the superconducting critical field H_c. The location of H_c in Fig. 16 has been roughly determined by looking at local densities (see Ref. 23 for the method) since Cooper pairs break down above this field. For larger U, the superconducting critical field is smaller. These results are also observed in the *t-J* model having in mind that $J/t \sim t/U$ (see Sec. IV E 2 and Fig. 19). For higher magnetization states, Gutzwiller projection induces a rather different behavior between strongly interacting systems (Hubbard $U=16$ and *t-J*), the Hubbard model with $U=8$ which displays the expected square-root-like behaviors near critical fields in good agreement with the band-emptying scenario proposed in Sec. IV C. At last, a quick comparison with the isotropic noninteracting system proves the nontrivial role of interactions in the apparition of these plateaus.

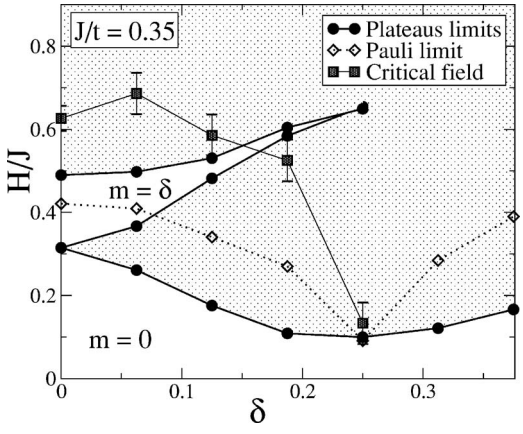

FIG. 17. Phase diagram for the isotropic two-leg *t-J* ladder in the (H,δ) plane for $J/t=0.35$. The large FFLO phase is delimited by the upper limit of the $m=0$ plateau and the critical field H_c. Note also that in this part of the diagram, the $m=\delta$ phase is not expected to be a superconducting phase but rather metallic.

The magnetic part of the phase diagram of the *t-J* model with $J/t=0.35$ has been computed (see Fig. 17) and is very similar to the one obtained with $J/t=0.5$ (see Ref. 23) but have larger $m=\delta$ plateaus. We propose that such a phase diagram is generic for the isotropic *t-J* and Hubbard models under Zeeman effect at low doping and for parameters $0.25 \lesssim (J/t \sim 4t/U) \lesssim 1.0$ corresponding to the strong-coupling regime. Varying J/t modifies the width of the different phases as proposed in Fig. 19. Lastly, we note that $\delta=1/4$ corresponds to the end of the plateau both for $J/t=0.35$ and $J/t=0.5$. Furthermore, the magnetization curves are strongly modified with $\delta>1/4$ (data not shown), which suggests that this hole density corresponds to a singular point.

2. Charge gaps and exceeding of the Pauli limit

To study the charge degree of freedom of the system, we computed the two-particle gap Δ_{2p} (related to the inverse compressibility) and pairing energy Δ_p as a function of the magnetization m to discuss the nature of the ground state. With n_h the number of holes and S^z the total spin along the magnetic field, we have the definitions

$$\Delta_{2p}(S^z) = E(n_h+2,S^z) + E(n_h-2,S^z) - 2E(n_h,S^z) \quad (32)$$

and

$$\Delta_p(S^z) = E(n_h-1,S^z+1/2) + E(n_h-1,S^z-1/2) - E(n_h,S^z) - E(n_h-2,S^z). \quad (33)$$

The evolution of these gaps under increasing magnetization is displayed in Fig. 18. Superconducting correlations are also algebraic when the pairing energy is finite from Fig. 6 of Ref. 23. These observations confirm that the system is in a superconducting state, except in the $m=\delta$ plateau where a finite two-particle charge gap is found as well as a strong reduction of all superconducting correlations from Fig. 6 of Ref. 23. However, the field $\phi_{\uparrow}^{+}$ remains gapless in the irrational plateau, while other fields are gapful. This suggests that the system is in a metallic phase in this plateau phase. Increasing the magnetic field brings the system back into a superconducting phase, giving an example of reentrant superconductivity which shares similarity with a proposal for a bilayer system.[45] The finite value of Δ_{2p} in the thermodynamic limit within the plateau phase can be inferred by using Eq. (32) and the constraint $m=\delta$ for continuous values of hole doping, which are more general hypotheses than the particular case under study. Indeed, it is straightforward to find that it exactly equals the width $E(n_h,S^z+1)-E(n_h,S^z-1)$ of the plateau in the thermodynamical limit. This is co-

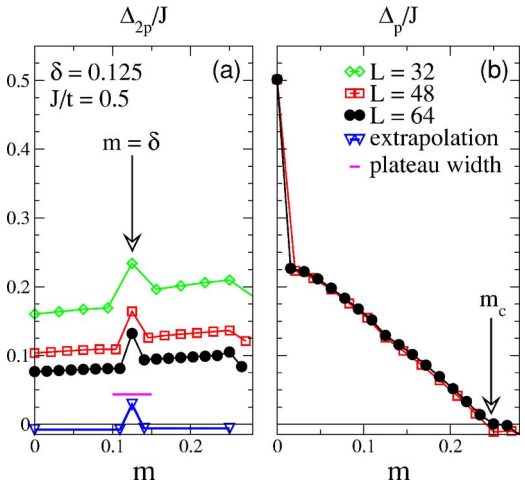

FIG. 18. (Color online) (a) Two-particle gap and (b) pairing energy for isotropic ladders as a function of magnetization. An anomaly in the two-particle gap at $m=\delta$ is clearly visible, while the pairing energy remains finite up to the superconducting-metallic state transition. m_c represents the magnetization corresponding to the superconducting critical field H_c.

herent with the numerical results of Fig. 18 obtained at fixed δ. It simply means that removing a hole pair in a system which has $m=\delta$ (i.e., the same number of hole pairs and magnons) is energetically equivalent to adding a magnon in a system with $m'=\delta'$ at a slightly lower density. Thus, one has to pay the energy gap of the $m'=\delta'$ plateau for that, and this gap equals the $m=\delta$ gap in the thermodynamical limit.

We now come to the computation of the theoretical Pauli limit H_P and of the actual superconducting critical field H_c. The Pauli limit is defined by equaling the condensation energy at $T=0$ and $H=0$ to the energy of the electrons coming from a broken pair and stabilized by Zeeman effect.[4] We have access numerically to the condensation energy of a pair of electrons at zero magnetization through $\Delta_p(S^z=0)$. Paired electrons in a singlet state do not take advantage of Zeeman effect contrary to unpaired electrons which can be polarized along the magnetic field. The total energy of these two electrons is $2E(n_h-1,+1/2)-2\times\frac{1}{2}\times H$, to be compared with the total energy of the same system with paired electrons, $E(n_h,0)+E(n_h-2,0)$. By looking at Eq. (33) with $S^z=0$, we find that the Pauli field simply reads $H_P=\Delta_P(S^z=0)$. What actually occurs in the system is a transition to a FFLO state which changes the nature of the ground state so that the Pauli limit can be exceeded. The superconducting upper critical field is deduced from the location at which $\Delta_p(S^z)$ crosses zero, which gives a critical magnetization m_c and in turn the critical field H_c reported in Fig. 17. It is important to note that these calculations are exact and with no approximation. The superconducting critical field H_c can also be interpreted in the bosonization language as the emptying of the $(\pi,\downarrow)$ band (see Sec. IV C). From Figs. 17 and 19, it is clear that Pauli limit is exceeded at low doping and for a wide region of parameters. This exceeding of the Pauli limit can be associated with the FFLO mechanism discussed in Sec. IV D from the behavior of the superconducting correlations.

At last, we remark from Fig. 18 that the pairing energy has a discontinuity upon magnetizing the ladder (in the $m\to 0$ limit) very similar to the known discontinuity of the spin gap[46,47] upon doping the ladder (in the $\delta\to 0$ limit). Note also that the strong reduction of the pairing energy and of the spin gap for $\delta=1/4$ observed in Fig. 17 is related to the proximity of the CDW phase,[16] which occurs for $J/t\sim 0.2$.

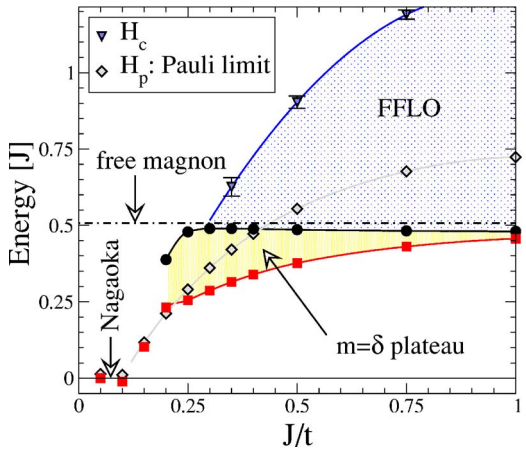

FIG. 19. (Color online) H_c, H_P, and $m=\delta$ plateau on an isotropic two-leg t-J ladder doped with two holes as a function of J/t (this corresponds to the $\delta\to 0$ limit of the phase diagram of Fig. 17). The curve with squares corresponds to the upper limit of the $m=0$ plateau and the lower limit of the $m=\delta$ plateau, while the curve with circles to the upper limit of the $m=\delta$ plateau. The FFLO phase is delimited by the curve with circles and the curve with triangles. Results are extrapolated from DMRG results on systems with $L=32,48,64$. For small J/t, a Nagaoka phase is found but because of strong finite-size effects, we do not discuss this part of the diagram. Lines are guides for the eyes.

3. Phase diagram

The phase diagram of Fig. 17 is proposed to be generic in the coupled-band regime for strong repulsive interactions. In addition to the magnetic properties described above, the system is in a LE superconducting state in the $m=0$ plateau, in a Luttinger liquid superconducting phase below H_c, and in a metallic phase in the $m=\delta$ plateau phase. Above H_c, the system switches to a metallic phase with three ungapped sectors which couple both spin and charge degrees of freedom. The central charge c is expected to take the following values in each phase encountered as the magnetic field is increased (taking, for example, a vertical cut in Fig. 17 with $\delta=0.063$): $c=1$ ($m=0$ plateau), 2 (FFLO below the $m=\delta$ plateau), 1 ($m=\delta$ plateau), 2 (FFLO above the $m=\delta$ plateau), and 3 (above H_c), 2 (saturation phase). Note that one could expect a last transition $c=2\to 1$ for certain parameters, corresponding to a situation where the $(0,\uparrow)$ is completely filled. Since such a transition would induce a cusp in the magnetization curve and there is no sign of it in Fig. 16, we conclude that $c=2$ is the value for the saturation in this regime.

To evaluate the role of J/t on this generic phase diagram, we computed various energy gaps and critical fields in the $\delta\to 0$ limit, i.e., for two holes on a ladder with $L\to\infty$. Results are extrapolated from systems of length $L=32,48,64$ and are displayed in Fig. 19. First, we note that for very small J/t, a Nagaoka phase competes with the LE phase and

induces strong finite-size effects in the ground states; thus, the displayed boundary between these phases *does not* correspond to the thermodynamical transition. Hence, we only focus on points for which the LE phase is stable (on finite-size systems), which are found to be qualitatively for $0.25 \leqslant J/t \leqslant 1.0$. For large J/t, the model undergoes a phase separation between holes and spins and we are not interested in the behavior near this instability. In this region of parameters, we have the following behavior: the width of the plateau increases for decreasing J/t (for $J/t=1.0$, the $m=\delta$ plateau is hardly visible at finite density, data not shown), while the exceeding of the Pauli limit increases with J/t (which simply follows the increase of the pairing energy).

These elementary excitation gaps at $\delta \to 0^+$ can be related to the dynamics of the system[47] when $m=0$. The difference between $\min(\Delta_p, \Delta_M)$ and the spin gap corresponds to the binding energy of the resonant magnetic mode. It is interesting to note that the upper limit of the $m=\delta$ plateau is approximately independent of J/t and corresponds to a free magnon (which is nothing but the spin gap of the undoped system $\Delta_M \sim J/2$). Indeed, once the hole pair is bound to a magnon, the next magnetic excitation is to create a magnon in the remaining undoped background, which cost is Δ_M, slightly renormalized by the scattering with the hole-magnon bound state. This supports the phenomenological mechanism proposed in Ref. 23 for the opening of the irrational plateau. The binding of the hole pair to the magnon comes from the gain in kinetic energy holes have in a locally ferromagnetic environment. It is thus expected that the binding energy increases with t/J. It is also likely to find such a bound state in the vicinity of a Nagaoka phase which here competes with the LE phase. It also explains the decrease of the pairing energies as J/t is reduced. Note that previous studies of this resonant magnetic mode with exact diagonalization[47] and periodic boundary conditions agree with these results, and hence suggest that open boundary conditions do not affect this generic phase diagram.

V. COUPLED-CHAIN REGIME

A. Dominant exchange model

By strongly reducing the interchain hopping amplitude, one can reach the coupled-chain regime in which interchain hopping is an irrelevant perturbation[48–51] and the relevant interchain couplings are either the Josephson coupling (for attractive intrachain interactions) or the exchange coupling (for repulsive interchain interaction). An important point is that even if the bare model has only interchain hopping, Josephson and exchange couplings are generated by the renormalization group (RG) flow[49–51] and, as a result, the effective model always contains this type of interaction. In the rest of the paper, we will call this strong-coupling limit the "chain representation." The bosonized Hamiltonian describing the two uncoupled chains reads[39]

$$\mathcal{H} = \sum_{\substack{i=1,2 \\ \nu=\rho,\sigma}} \int \frac{dx}{2\pi} \left[u_\nu K_\nu (\pi \Pi_{\nu,i})^2 + \frac{u_\nu}{K_\nu} (\partial_x \phi_{\nu,i})^2 \right], \quad (34)$$

where we have dropped terms $\propto g_{1\perp} \cos \sqrt{8} \phi_{\sigma,i}$ since these terms are marginally irrelevant in the case of repulsive interactions. In the case of attractive interactions, they also become irrelevant upon the application of a magnetic field strong enough to induce a C-IC transition.[43]

1. Dominant exchange

For small $J_\parallel/t_\parallel$ ratios, the analysis of the scaling dimensions in the t-J model on a single chain[52] shows that the dominant interchain coupling is the exchange one. This term reads

$$\frac{2J_\perp \alpha}{(2\pi\alpha)^2} \cos \sqrt{2}(\phi_{\rho,1} - \phi_{\rho,2}) \times \left[\cos \sqrt{2}(\theta_{\sigma,1} - \theta_{\sigma,2}) + \frac{1}{2} \cos \sqrt{2}(\phi_{\sigma,1} - \phi_{\sigma,2}) + \frac{1}{2} \cos \sqrt{2}(\phi_{\sigma,1} + \phi_{\sigma,2} + 2\pi m x) \right], \quad (35)$$

where we have the usual definition $\theta_{\nu,i} = \int \pi \Pi_{\nu,i}$. For nonzero magnetization, the last term is oscillating and drops from the Hamiltonian. It is convenient to introduce the new fields

$$\phi_{\nu,\pm} = \frac{1}{\sqrt{2}}(\phi_{\nu,1} \pm \phi_{\nu,2}), \quad \theta_{\nu,\pm} = \frac{1}{\sqrt{2}}(\theta_{\nu,1} \pm \theta_{\nu,2}).$$

With this transformation, the exchange term is rewritten as

$$\frac{2J_\perp}{(2\pi\alpha)^2} \int dx \cos 2\phi_{\rho-} \left[\cos 2\theta_{\sigma-} + \frac{1}{2} \cos 2\phi_{\sigma-} \right]. \quad (36)$$

Moreover, the two chains being equivalent, the chain Hamiltonian is rewritten as

$$\mathcal{H} = \sum_{\substack{r=\pm \\ \nu=\rho,\sigma}} \int \frac{dx}{2\pi} \left[u_\nu K_\nu (\pi \Pi_{\nu,r})^2 + \frac{u_\nu}{K_\nu} (\partial_x \phi_{\nu,r})^2 \right]. \quad (37)$$

Obviously, the Hamiltonians describing the fields $\phi_{\sigma+}$ and $\phi_{\rho+}$ are purely quadratic, indicating that the total charge and the total spin excitations are gapless. The fields $\phi_{\sigma-}$ and $\phi_{\rho-}$ are described by a generalized sine Gordon model. The sine Gordon interaction term (36) can be treated within a RG analysis. The scaling dimension of the term $\cos 2\phi_{\rho-} \cos 2\theta_{\sigma-}$ is $K_{\rho-} + K_{\sigma-}^{-1}$ and scaling dimension of the term $\cos 2\phi_{\rho-} \cos 2\phi_{\sigma-}$ is $K_{\rho-} + K_{\sigma-}$. From the analysis of Ref. 30, we can conclude that in the case of interest we have $K_{\sigma-} > 1$ and $\cos 2\phi_{\rho-} \cos 2\theta_{\sigma-}$ is the most relevant term and for antiferromagnetic $J_\perp$ the ground state has $\langle \phi_{\rho-} \rangle = 0 \pmod{\pi}$ and $\langle \theta_{\sigma-} \rangle = \frac{\pi}{2} \pmod{\pi}$.

2. Most divergent superconducting fluctuations

The expression of the intrachain order parameters in terms of the fields in Eq. (37) can be found in Ref. 39. When reexpressed in terms of the $\pm$ fields and denoting $q = \pi m$, the singlet operator reads

$$O_{SS,i} = \sum_{\sigma} \sigma e^{iq\sigma x} \psi_{R,i,\sigma} \psi_{L,i,-\sigma} \sim \sum_{\sigma} \sigma e^{iq\sigma x} e^{i[\theta_{\rho+} - (-)^i \theta_{\rho-}]} e^{-i\sigma[\phi_{\sigma+} - (-)^i \phi_{\sigma-}]}, \quad (38)$$

and, for triplet operators, we have

$$O_{TS,i,S^z=0} = \sum_{\sigma} e^{iq\sigma x} \psi_{R,i,\sigma} \psi_{L,i,-\sigma} \sim \sum_{\sigma} e^{iq\sigma x} e^{i[\theta_{\rho+} - (-)^i \theta_{\rho-}]} e^{-i\sigma[\phi_{\sigma+} - (-)^i \phi_{\sigma-}]}, \quad (39)$$

$$O_{TS,i,S^z=1} = \psi_{R,i,\uparrow} \psi_{L,i,\uparrow} \sim e^{i[\theta_{\rho+} - (-)^i \theta_{\rho-}]} e^{-i[\theta_{\sigma+} - (-)^i \theta_{\sigma-}]}. \quad (40)$$

For the interchain operators, the singlet operator reads

$$O'_{SS} = \sum_{\sigma} \sigma e^{iq\sigma x} \psi_{R,1,\sigma} \psi_{L,2,-\sigma} \sim \sum_{\sigma} \sigma e^{iq\sigma x} e^{i[\theta_{\rho+} - \phi_{\rho-} + \sigma(\theta_{\sigma-} - \phi_{\sigma+})]}, \quad (41)$$

while the triplet ones read

$$O'_{TS,S^z=0} = \sum_{\sigma} e^{iq\sigma x} \psi_{R,1,\sigma} \psi_{L,2,-\sigma} \sim \sum_{\sigma} e^{iq\sigma x} e^{i[\theta_{\rho+} - \phi_{\rho-} + \sigma(\theta_{\sigma-} - \phi_{\sigma+})]}, \quad (42)$$

$$O'_{TS,S^z=1} = \psi_{R,1,\uparrow} \psi_{L,2,\uparrow} \sim e^{i(\theta_{\rho+} - \phi_{\rho-} + \theta_{\sigma+} - \phi_{\sigma-})}. \quad (43)$$

Since $\langle \phi_{\rho-} \rangle = 0$, we have $\langle e^{i\phi_{\rho-}} \rangle \neq 0$ and by duality $\langle e^{i\theta_{\rho-}(x)} e^{i\theta_{\rho-}(0)} \rangle \sim e^{-x/\xi_-}$. This property implies that all the intrachain superconducting correlations should decay exponentially along the chains. On the other hand, the interchain correlations are reinforced. The physical picture is that in this situation, fermions of opposite spins on each chain are bound together by the exchange interaction. Whether the dominant superconductivity is the interchain one or the intrachain one depends on the value of $K_{\sigma-}$. Since we have $K_{\sigma-} > 1$ in our case, the dominant superconducting correlations are the interchain singlet and the interchain triplet $S^z = 0$. Note that these two operators have exactly the same critical exponents. In the case of dominant Josephson coupling, the situation is reversed.

3. $S^z = 1$ triplet with a $2k_F$ momentum

It is also straightforward to derive an expression of the operator $e^{2ik_{F,\sigma}x} \psi_{R,1,\sigma} \psi_{R,2,\sigma}$ associated with the $2k_F$ triplet correlations. This expression reads

$$e^{2ik_{F,\sigma}x} e^{i(\theta_{\rho+} - \phi_{\rho+})} e^{i\sigma(\theta_{\sigma+} - \phi_{\sigma+})}. \quad (44)$$

This expression again shows power-law correlations with the critical exponent

$$\frac{1}{2}(K_{\rho+} + K_{\rho+}^{-1} + K_{\sigma+} + K_{\sigma+}^{-1}) \quad (45)$$

very similar to what has been obtained in Sec. IV B 2.

TABLE III. The different dominant superconducting fluctuations with the associated critical exponents. Josephson coupling dominates for $K_{\rho-} > 1$ and exchange coupling dominates for $K_{\rho-} < 1$.

Dominant interaction	Dominant superconducting correlations	Critical exponent
Exchange coupling ($K_{\sigma-} > 1$)	Rung singlet and rung triplet $S^z = 0$	$\frac{1}{2K_{\rho+}} + \frac{K_{\sigma+}}{2}$
Josephson coupling ($K_{\sigma-} > 1$)	Leg triplet $S^z = 1$	$\frac{1}{2K_{\rho+}} + \frac{1}{2K_{\sigma+}}$

B. Favoring the Josephson coupling in the coupled-chain regime

Let us consider the regime of small interchain hopping and assume that now the intrachain terms are such that $J_{\parallel} \sim 4t_{\parallel}$. In this case, the dominant term becomes the Josephson coupling[52] and the perturbation term [Eq. (36)] is replaced by

$$\frac{2\lambda\alpha}{(2\pi\alpha)^2} \cos\sqrt{2}(\theta_{\rho,1} - \theta_{\rho,2}) \times \left[\cos\sqrt{2}(\theta_{\sigma,1} - \theta_{\sigma,2}) + \frac{1}{2}\cos\sqrt{2}(\phi_{\sigma,1} - \phi_{\sigma,2}) + \frac{1}{2}\cos\sqrt{2}(\phi_{\sigma,1} + \phi_{\sigma,2} + 2\pi m x) \right]. \quad (46)$$

The treatment parallels the one of the exchange coupling in Sec. V A 1. The Josephson term is rewritten in the form

$$\frac{2\lambda}{(2\pi\alpha)^2} \int dx \cos 2\theta_{\rho-} \left[\cos 2\theta_{\sigma-} + \frac{1}{2}\cos 2\phi_{\sigma-} \right]. \quad (47)$$

The scaling dimension of the term $\cos 2\theta_{\rho-} \cos 2\theta_{\sigma-}$ is $K_{\rho-}^{-1} + K_{\sigma-}^{-1}$ and scaling dimension of the term $\cos 2\phi_{\rho-} \cos 2\phi_{\sigma-}$ is $K_{\rho-}^{-1} + K_{\sigma-}$. A RG analysis similar to the one inSec. V A 1 yields for $K_{\sigma-} > 1$ $\langle \theta_{\rho-} \rangle = 0 \pmod{\pi}$ and $\langle \theta_{\sigma-} \rangle = \frac{\pi}{2} \pmod{\pi}$ and for $K_{\sigma-} > 1$ $\langle \theta_{\rho-} \rangle = 0 \pmod{\pi}$ and $\langle \phi_{\sigma-} \rangle = \frac{\pi}{2} \pmod{\pi}$. This time, interchain correlations are decaying exponentially, and the dominant superconducting correlations are the intrachain ones. Since $K_{\sigma-} > 1$, $\langle \theta_{\sigma-} \rangle = \frac{\pi}{2}$ and the intrachain $S^z = 1$ triplet superconductivity is dominant. For $K_{\sigma-} < 1$, the dominant superconducting correlations are the intrachain singlet and intrachain triplet $S^z = 0$.

The results are summarized in Table III where the critical exponents η_α are defined by $\langle O_\alpha(x) O_\alpha(0) \rangle \sim |x|^{-\eta_\alpha}$. We note that triplet $S^z = 1$ superconducting correlations can never coexist with singlet superconducting correlations.

We have tried to observe these predictions numerically but using both the t-J model with small $t_\perp$, $J_\perp$ and Hubbard model with small $t_\perp$. Unfortunately, for large $J_{\parallel}/t_{\parallel}$, the system with open boundary conditions has edge effects due to the proximity of the phase separation which occurs generically in the t-J model for large J/t. When edge effects are absent and in the Hubbard model, we did not find evidence

of the proposed predictions, i.e., we mostly found cases related to the coupled-band regime fixed point. Still, contrary to the isotropic case which has been widely studied numerically at zero magnetization, a systematic study of the phase diagram at zero magnetization would be necessary before tackling the system under magnetic field. This systematic study is out of the scope of the present paper.

VI. CONCLUSION

In conclusion, we studied the case of two fermionic coupled chains, or ladders, under a magnetic field inducing a Zeeman effect in the system. The first situation we addressed was the free and strong-coupling limits. We found that large doping-dependent magnetization plateaus occur for "coupled-dimer" systems (with large interactions on the rungs) and that pairing is not expected in the $m=\delta$ magnetization plateau phase. For a system with isotropic couplings, we showed that $m=\delta$ plateaus also exist and pairing survives to much higher magnetizations. Furthermore, the computation of the one- and two-particle gap and bosonization interpretation proved that the plateau phase is metallic, while the system is in a superconducting state below and above this plateau. In addition, we computed the superconducting upper critical field which is much larger than the Pauli limit for a wide range of the parameters of the t-J model. Superconducting correlation functions precisely agree with the bosonization predictions up to the accuracy of our methods. Turning to the coupled-chain regime, other interesting unconventional behaviors are predicted for the superconducting correlations with, for instance, the possibility of having polarized triplet correlations under high magnetic fields. However, quick numerical investigation studies were not able to find good parameters providing evidence of such predictions.

Discussion on experiments. We now briefly discuss consequences for experiments. First of all, the possibility of measuring irrational magnetization plateau would give a direct access to the hole doping δ which has recently been estimated[53] to be $\delta\sim 0.1$ in the superconducting phase of doped ladders. However, the magnetization is a global measurement including the contribution of all subsystems. For instance, the magnetization curve of SCCO has very recently been measured,[54] showing that the main contribution comes from the chain subsystem. On the other hand, measurements such as NMR under high magnetic field can provide local information on each subsystem.

The superconducting critical field $H_c(T)$ of SCCO has been measured under high pressure[20,21] and displays a strong anisotropy and an anomalous $H_c(T)$ curvature. Furthermore, $H_c(T)$ much larger than the standard Pauli limit are found, suggesting an exceeding of the latter. The nature of the superconductivity in SCCO is a long-standing debate because of its complex structure and the requirement of high-pressure experiments. Questions such as the nature of the pairing or the dimensionality of superconductivity have not reached full agreement yet. One possibility is that superconducting fluctuations of the RVB type develop in the ladder subsystem, leading to true superconducting order once these ladders are coupled through Josephson coupling (T_c being controlled by this coupling rather than by the magnetic energy scale J). In this case, our study suggests that the FFLO mechanism is relevant at the ladder subsystem level and thus could be stabilized when coupling the ladders. The other possibility would be that the superconducting phase is really two-dimensional,[55,56] allowing other explanations of the exceeding of Pauli limit such as triplet pairing[21] *when* $H=0$. NMR measurements[57] also showed that superconductivity survives under rather high field and p-wave superconductivity was suggested. Note that our study also proposes the possibility for the emergence at high fields of pairing channels not present at $H=0$ since magnetic fluctuations from which pairing originates are strongly affected by the magnetic field. Lastly, we mention that anomalous curvature of $H_c(T)$ as found in experiments was predicted in the mean-field approach of FFLO states in quasi-one- and two-dimensional d-wave superconductors.[4]

ACKNOWLEDGMENTS

G.R. would like to thank IDRIS (Orsay, France) and CALMIP (Toulouse, France) for use of supercomputer facilities. G.R., P.P., and D.P. thank Agence Nationale de la Recherche (France) for support.

*Electronic address: roux@irsamc.ups-tlse.fr
†Electronic address: edmond.orignac@ens-lyon.fr

[1] P. Fulde and R. A. Ferrell, Phys. Rev. **135**, A550 (1964); A. I. Larkin and Y. N. Ovchinnikov, Sov. Phys. JETP **20**, 762 (1965); R. Casalbuoni and G. Nardulli, Rev. Mod. Phys. **76**, 263 (2004).
[2] T. Ishiguro, *High Magnetic Fields*, Lecture Notes in Physics, Vol. 595 (Springer, Heidelberg, 2002).
[3] N. Dupuis, Phys. Rev. B **51**, 9074 (1995).
[4] H. Shimahara and D. Rainer, J. Phys. Soc. Jpn. **66**, 3591 (1997).
[5] M. Sigrist, *Lectures on the Physics of Correlated Electron Systems IX: Ninth Training Course in the Physics of Correlated Electron Systems and High-Tc Superconductors*, edited by A. Avella and F. Mancini, AIP Conf. Proc. No. 789 (AIP, New York, 2005), p. 165.
[6] E. Dagotto and T. M. Rice, Science **271**, 618 (1996); T. M. Rice, Z. Phys. B: Condens. Matter **103**, 165 (1997); E. Dagotto, Rep. Prog. Phys. **62**, 1525 (1999).
[7] D. C. Cabra, A. Honecker, and P. Pujol, Phys. Rev. Lett. **79**, 5126 (1997); Phys. Rev. B **58**, 6241 (1998).
[8] G. Chaboussant, M.-H. Julien, Y. Fagot-Revurat, L. P. Lévy, C. Berthier, M. Horvatić, and O. Piovesana, Phys. Rev. Lett. **79**, 925 (1997); G. Chaboussant, Y. Fagot-Revurat, M.-H. Julien, M. E. Hanson, C. Berthier, M. Horvatić, L. P. Lévy, and O. Piovesana, *ibid.* **80**, 2713 (1998).
[9] B. C. Watson, V. N. Kotov, M. W. Meisel, D. W. Hall, G. E. Granroth, W. T. Montfrooij, S. E. Nagler, D. A. Jensen, R.

Backov, M. A. Petruska, G. E. Fanucci, and D. R. Talham, Phys. Rev. Lett. **86**, 5168 (2001).
[10] C. P. Landee, M. M. Turnbull, C. Galeriu, J. Giantsidis, and F. M. Woodward, Phys. Rev. B **63**, 100402(R) (2001).
[11] H. Frahm and C. Sobiella, Phys. Rev. Lett. **83**, 5579 (1999).
[12] D. C. Cabra, A. De Martino, A. Honecker, P. Pujol, and P. Simon, Phys. Lett. A **268**, 418 (2000).
[13] D. C. Cabra, A. De Martino, A. Honecker, P. Pujol, and P. Simon, Phys. Rev. B **63**, 094406 (2001).
[14] C. A. Hayward, D. Poilblanc, R. M. Noack, D. J. Scalapino, and W. Hanke, Phys. Rev. Lett. **75**, 926 (1995).
[15] E. Orignac and D. Poilblanc, Phys. Rev. B **68**, 052504 (2003); D. Poilblanc, D. J. Scalapino, and S. Capponi, Phys. Rev. Lett. **91**, 137203 (2003); D. Poilblanc and D. J. Scalapino, Phys. Rev. B **71**, 174403 (2005).
[16] S. R. White, I. Affleck, and D. J. Scalapino, Phys. Rev. B **65**, 165122 (2002).
[17] P. W. Anderson, Science **235**, 1196 (1987).
[18] A. Gozar and G. Blumberg, *Frontiers in Magnetic Materials* (Springer-Verlag, Heidelberg, 2005), pp. 653–695.
[19] M. Uehara, T. Nagata, J. Akimitsu, H. Takahashi, N. Môri, and K. Kinoshita, J. Phys. Soc. Jpn. **65**, 2764 (1996); D. Jerome, P. Auban-Senzier, and Y. Piskunov, *High Magnetic Fields*, Lecture Notes in Physics, Vol. 595 (Springer, Heidelberg, 2002).
[20] D. Braithwaite, T. Nagata, I. Sheikin, H. Fujino, J. Akimitsu, and J. Flouquet, Solid State Commun. **114**, 533 (2000).
[21] T. Nakanishi, N. Motoyama, H. Mitamura, N. Takeshita, H. Takahashi, H. Eisaki, S. Uchida, and N. Mori, Phys. Rev. B **72**, 054520 (2005).
[22] M. Matsukawa, Y. Yamada, M. Chiba, H. Ogasawara, T. Shibata, A. Matsushita, and Y. Takano, Physica C **411**, 101 (2004).
[23] G. Roux, S. R. White, S. Capponi, and D. Poilblanc, Phys. Rev. Lett. **97**, 087207 (2006).
[24] S. R. White, Phys. Rev. Lett. **69**, 2863 (1992); Phys. Rev. B **48**, 10345 (1993).
[25] U. Schollwöck, Rev. Mod. Phys. **77**, 259 (2005).
[26] D. C. Cabra, A. De Martino, P. Pujol, and P. Simon, Europhys. Lett. **57**, 402 (2002).
[27] T. Pruschke and H. Shiba, Phys. Rev. B **46**, 356 (1992).
[28] K. Yang, Phys. Rev. B **63**, 140511(R) (2001).
[29] M. Yamanaka, M. Oshikawa, and I. Affleck, Phys. Rev. Lett. **79**, 1110 (1997); M. Oshikawa, M. Yamanaka, and I. Affleck, *ibid.* **78**, 1984 (1997); P. Gagliardini, S. Haas, and T. M. Rice, Phys. Rev. B **58**, 9603 (1998).
[30] N. Nagaosa, Solid State Commun. **94**, 495 (1995); N. Nagaosa and M. Oshikawa, J. Phys. Soc. Jpn. **65**, 2241 (1996).
[31] D. V. Khveshchenko and T. M. Rice, Phys. Rev. B **50**, 252 (1994).
[32] A. M. Finkelstein and A. I. Larkin, Phys. Rev. B **47**, 10461 (1993).
[33] H. J. Schulz, Phys. Rev. B **53**, R2959 (1996).
[34] L. Balents and M. P. A. Fisher, Phys. Rev. B **53**, 12133 (1996).
[35] M. Troyer, H. Tsunetsugu, and T. M. Rice, Phys. Rev. B **53**, 251 (1996).
[36] M. Fabrizio, Phys. Rev. B **48**, 15838 (1993).
[37] H. Frahm and V. E. Korepin, Phys. Rev. B **42**, 10553 (1990); **43**, 5653 (1991).
[38] E. Orignac and Y. Suzumura, Eur. Phys. J. B **23**, 57 (2001).
[39] T. Giamarchi, *Quantum Physics in One Dimension*, International Series of Monographs on Physics, Vol. 121 (Oxford University Press, Oxford, 2004).
[40] R. Konik, F. Lesage, A. W. W. Ludwig, and H. Saleur, Phys. Rev. B **61**, 4983 (2000).
[41] H. Schulz, arXiv:cond-mat/9808167 (unpublished).
[42] S. R. White, Phys. Rev. B **72**, 180403(R) (2005).
[43] G. I. Dzhaparidze and A. A. Nersesyan, JETP Lett. **27**, 334 (1978); V. L. Pokrovsky and A. L. Talapov, Phys. Rev. Lett. **42**, 65 (1979); H. J. Schulz, Phys. Rev. B **22**, 5274 (1980).
[44] E. Jeckelmann, D. J. Scalapino, and S. R. White, Phys. Rev. B **58**, 9492 (1998).
[45] A. Buzdin, S. Tollis, and J. Cayssol, Phys. Rev. Lett. **95**, 167003 (2005).
[46] H. H. Lin, L. Balents, and M. P. A. Fisher, Phys. Rev. B **58**, 1794 (1998).
[47] D. Poilblanc, O. Chiappa, J. Riera, S. R. White, and D. J. Scalapino, Phys. Rev. B **62**, 014633 (2000); D. Poilblanc, E. Orignac, S. R. White, and S. Capponi, *ibid.* **69**, 220406(R) (2004).
[48] X. G. Wen, Phys. Rev. B **42**, 6623 (1990).
[49] D. Boies, C. Bourbonnais, and A.-M. S. Tremblay, in *Proceedings of the XXXIst Rencontres de Moriond*, edited by T. Martin, G. Montambaux, and J. Tran Thanh Van (Éditions Frontières, Gif sur Yvette, 1996).
[50] V. M. Yakovenko, JETP Lett. **56**, 510 (1992).
[51] S. Brazovskii and V. Yakovenko, J. Phys. (Paris), Lett. **46**, L111 (1985).
[52] M. Ogata, M. U. Luchini, S. Sorella, and F. F. Assaad, Phys. Rev. Lett. **66**, 2388 (1991).
[53] Y. Piskunov, D. Jérome, P. Auban-Senzier, P. Wzietek, and A. Yakubovsky, Phys. Rev. B **72**, 064512 (2005).
[54] R. Klingeler, N. Tristan, B. Buchner, M. Hucker, U. Ammerahl, and A. Revcolevschi, Phys. Rev. B **72**, 184406 (2005); R. Klingeler, B. Buchner, K. Y. Choi, V. Kataev, U. Ammerahl, A. Revcolevschi, and J. Schnack, *ibid.* **73**, 014426 (2006).
[55] T. Nagata, M. Uehara, J. Goto, J. Akimitsu, N. Motoyama, H. Eisaki, S. Uchida, H. Takahashi, T. Nakanishi, and N. Môri, Phys. Rev. Lett. **81**, 1090 (1998).
[56] Y. Piskunov, D. Jérome, P. Auban-Senzier, P. Wzietek, and Y. Yakubovsky, Phys. Rev. B **69**, 014510 (2004); N. Motoyama, H. Eisaki, S. Uchida, N. Takeshita, N. Môri, T. Nakanishi, and H. Takahashi, Europhys. Lett. **58**, 758 (2002).
[57] N. Fujiwara, N. Môri, Y. Uwatoko, T. Matsumoto, N. Motoyama, and S. Uchida, Phys. Rev. Lett. **90**, 137001 (2003); J. Phys.: Condens. Matter **17**, S929 (2005).